Dalton Transactions

Stereoelectronic Control of Photophysics: Red and Yellow Axial and Equatorial Anomers of a Rhenium-Quinoline Complex

Journal:	*Dalton Transactions*
Manuscript ID:	DT-COM-06-2015-002136
Article Type:	Communication
Date Submitted by the Author:	05-Jun-2015
Complete List of Authors:	Platel, Rachel; Lancaster University, Department of Chemistry Coogan, Mike; University of Lancaster, Chemistry Platts, James; Cardiff University, School of Chemistry

13th June 2015

Justification for Publication in *Dalton Transactions*

Please find attached a manuscript entitled "Stereoelectronic Control of Photophysics: Red and Yellow Axial and Equatorial Anomers of a Rhenium-Quinoline Complex" for consideration for publication in *Dalton Transactions*.

We report the synthesis and characterization of a novel hexahydropyrimidine ligand and two different rhenium species formed upon reaction of the ligand with $Re(CO)_5Br$. Importantly, both the optical and photophysical properties of these two complexes are different, and we have shown that an unusual feature of the stereochemistry of the complexes is responsible for this.

We believe that the manuscript warrants publication in *Dalton Transactions* for a number of reasons: the synthesis of a novel ligand, with the potential to be used with a range of metals; the clean formation of 2 rhenium anomers, which differ in their photophysical properties; the fact that we have been able to rationalise these differences in behaviour by DFT calculations and consideration of the electronic nature of the complexes. The multi-faceted nature of work means that it is likely to be of interest to a broad inorganic chemistry readership: to those with interests in fundamental coordination chemistry, spectroscopy and luminescence and molecular materials. Beyond its relevance to researchers in these areas we believe that the extremely unusual correlation of stereoelectronic structure and luminescence adds the exceptional 'twist' that merits urgent communication.

Having taken into account the comments and recommendations of referees from peer review from previous submission, we now submit a revised manuscript to you for consideration, along with a response to the referees.

Thank you very much for your efforts in handling this manuscript. I look forward to hearing your decision in due course.

Yours sincerely,

Dr Rachel Platel

Department of Chemistry
Lancaster University
Lancaster
LA1 1AE
United Kingdom

Email: r.platel@lancaster.ac.uk
Telephone: +44 (0)1524 592557

Stereoelectronic Control of Photophysics: Red and Yellow Axial and Equatorial Anomers of a Rhenium-Quinoline Complex

Rachel H. Platel,*[a] Michael P. Coogan[a] and James A. Platts[b]

Response to Referees' Comments

Responses to specific comments are shown in italics

Referee: 1

1.The overlaid emission and excitation spectra in Figure 6 is mis-leading, the emission intensities of both complexes are concentration-dependent. Thus, the apparent more intense emission may be due to different concentrations. If the structure features are compared, it is better to show the normalized spectra.
We thank the reviewer for drawing this to our attention. We have modified Fig. 6 to show normalised spectra.
Also, is there a mistake on the label?
There is no mistake in the labelling of these spectra.
It is quite puzzling why the excitation spectrum of 3 has a better match with the emission spectrum of 2 and the excitation spectrum of 2 has a better match with the emission spectrum of 3.
The apparent match is not a classic 'mirror image' of vibrational structure in excitation and emission (which we often do not observe in these broad MLCT bands) but a coincidence of overlap of the complex multiple transitions between different states which contribute to these spectra.

2. P.3 the statement "non-coordinated ring N in 2 contribute significantly to the HOMO" is not correct. How significant in compared to dpi(Re).
*Whilst we accept that the HOMO contribution by the non-coordinated N in **2** is not significant in itself, we believe that the fact that there is a contribution to the HOMO in **2** is important. Therefore, the text has been revised as follows to reflect this:*
*Page 3, line 48 onwards: "The non-coordinated ring nitrogen N(2) in **2** contributes significantly to the HOMO, whereas it does not contribute significantly in **3**, indicating a contribution from distant units which appears to be under stereoelectronic control"*
*Now reads: "The most significant difference in orbital plots is that the non-coordinated ring nitrogen N(2) in **2** contributes to the HOMO, whereas it does not contribute in **3**, indicating a contribution from distant units which appears to be under stereoelectronic control"*

3. P.4, taking into the account of error in the X-ray crystallography, the very slight difference in the bonding parameters described in lines 10-15 are insignificant to be conclusive.
We believe that the statement about lone pair interactions in the complexes (lines 10-11, page 4) is relevant to our argument, but accept that the errors in the crystallographic data mean we cannot draw conclusions from the bond lengths. The text has been revised to reflect this:
Page 4, line 12 onwards:"… which is supported by the relative bond lengths observed crystallographically"
Now reads: "Small differences in the relevant bond lengths observed crystallographically are, however, within error"

4. P.4 line 15 and ESI figure, what assumptions have been used in adjusting the protonated spectrum. It is not easily understand why an increase in absorption intensity upon addition of triflic acid would lead to the loss in the absorption intensity in the adjusted spectrum.

Moreover, was there any control experiments carried out for complex 3. If it has been done, how was it different from the result of complex 2.
There were no assumptions made in adjusting the protonated spectrum , it was simply repositioned (following the expected red-shift and increase in intensity upon increasing polarity for a charge transfer band) so that the trace for protonated and unprotonated spectra were superimposed – this was simply to visually emphasise that the shoulder had disappeared upon protonation, and there was no intention to imply that numerical values could be obtained from the adjusted spectrum. 2 does not show the extra band in 3which disappears upon protonation of 3, hence there was not expected to be a change in the shape of the spectrum and the control was not run. In response to this question we have now run the control and , as expected, upon protonation 2 shows the same polarity-dependent red shift and increase in intensity as 3, but the low energy region remains the same shape and this spectrum is now included in the ESI for comparison.

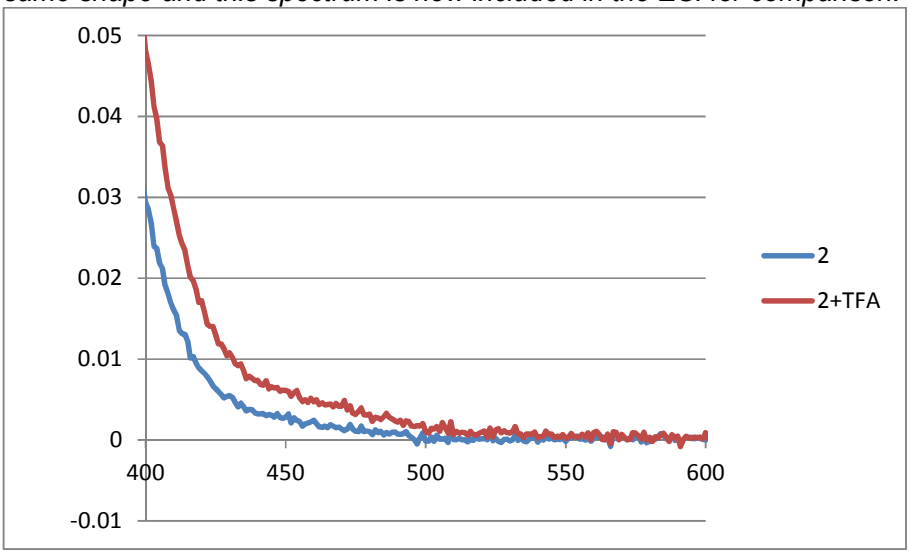

Referee: 2

-The sentence « if the excited state is located on one or both of the heterocycles » is not fully clear (do the authors mean : « the electronic density in the excited state is located… » ?) –
We agree this is not as clear as it could be. The text has been revised:
Page 1, line 33: "If the excited state is located…" now reads "If the electron density in the excited state…"

The sentence « Reductive amination of heterocyclic aldehydes with diamines, gives dimeric analogues of this unit (WHICH ONE? with pyridine, quinoline?) which could form stereochemically interesting complexes with 2 or 3 coordinated nitrogen atoms, with the possibility of fluxionality between these cases. » is not clear either.
We agree this lacks clarity. We intended to make the distinction between the Het^NR^Het, which would bind one metal, and an analogous Het^NRN^Het motif, that would have the potential to bind 2 metals. The text has been revised accordingly:
Page 1, line 39 onwards: "Reductive amination of heterocyclic aldehydes with diamines, gives dimeric analogues of this unit, which could form…" now reads: "Reductive amination of heterocyclic aldehydes with diamines, gives dimeric analogues of the isolated NR^Het unit (i.e. a Het^NRN^Het motif)…"

-Is the word anomer appropriate here?
The IUPAC definition of an anomer is "Diastereomers of glycosides, hemiacetals or related cyclic forms of sugars, or related molecules differing in configuration only at C-1 of an

aldose, C-2 of a 2-ketose, etc." We believe that compound 1 falls into the category of a related molecule, where C(10) is analogous to C1 in an aldose.

-page 3 « that these [transitions] are of significantly different strengths in the different isomers » May be of different probablity?
The word "strengths" has been replaced by the word "intensities"
Page 3 line 30: "these are of significantly different strengths in the different isomers." Now reads "these are of significantly different intensities in the different isomers."

-Can we be sure that the compounds 2 and 3 show the same structure in the solid state and in solution? I mean, is that possible that the bromide is lost with coordination of the pending quinoline? Is it possible to record UV-vis spectra in the solid form, to confirm that the same UV-vis spectra are obtained in the solid form and in solution are close?
The solution state structure of 2 and 3 is believed to be the same as in the solid state as the suggested solution state in which the bromine is lost with coordination of the quinolone would give a cationic complex which would, by analogy with literature examples, be expected to show absorption and emission bands which are considerably blue-shifted compared to these neutral species, as a result of the lowering of the ground state d- orbitals. More emphatically, the NMR shift of the methylene group of the quinolone is typically diagnostic, shifting downfield upon coordination. The (solution state) NMR shows little change in the values for these diastereotopic protons upon coordination, and additionally their relative positions do not change dramatically as would be expected if they became locked into a ring upon coordination (Ligand 1 : 3.80 (1H, d, $^2J_{HH}$ = 14.6 Hz, CH_2), 3.44 (1H, d, $^2J_{HH}$ = 14.6 Hz, CH_2) Complex 2: 2.91 (1H, d, $^2J_{HH}$ = 14.4 Hz, CH_2), 2.87 (1H, d, $^2J_{HH}$ = 14.4 Hz, CH_2) Complex 3: 4.42 (1H, d, $^2J_{HH}$ = 15.2 Hz, CH_2), 3.94 (1H, d, $^2J_{HH}$ = 15.2 Hz, CH_2),

-Could UV-visible spectra be calculated from the calculated energy of the OM? Even of not an exact match to the absolute experimental value, the difference in the energy of absorption between two structures can be easily discussed. This can be a nice proof that the position of the band is dependent on the presence of a contribution in N2 or not.
That would be a fully convincing rationalization. See [1] and [2]
[1] M. Obata, A. Kitamura, A. Mori, C. Kameyama, J.A. Czaplewska, R. Tanaka, I. Kinoshita, T. Kusumoto, H. Hashimoto, M. Harada, Y. Mikata, T. Funabikig, S. Yano, Dalton Trans (2008) 3292–3300.
[2] H.C. Bertrand, S. Clède, R. Guillot, F. Lambert, C. Policar, Inorg. Chem. 53 (2014) 6204-6223.
We thank the referee for this excellent suggestion. From the DFT calculations we have simulated the UV-vis spectra and these show that the observed low energy shoulder in compound 3 matches the calculated transition in which the participation of N2 is implicated. As sentence to this effect has been added to the manuscript, the simulated spectra added to the ESI and the suggested references also used:
*Page 4, line 19: "Furthermore, simulated UV-vis spectra from the DFT calculations show that the observed low energy shoulder in **3** matches the calculated transition in which the participation of the non-coordinated ring nitrogen is implicated (see ESI)."*

Referee: 3 (adjudicator)

Comments to the Author
This is a thorough and well-done piece of work but I agree with referee 1 that the modest difference in photophysical properties associated with the different coordination geometries of the bidentate ligand constitute 'control'. The observation lacks the high importance or generality required for publication in Chem. Comm.

However I think that the paper will be of sufficient interest to inorganic chemists to justify publication in Dalton Transactions as a communication following the minor corrections requested by both referees.

I note that referee 1 - the more critical of the first two - makes some comments which I do not believe to be justified. The referee claims that there cannot be a significant difference between the colours of the complexes based on the similarity of their absorption spectra and that the difference must be some sort artefact arising form differences in concentration. I know from experience that apparently minute changes in absorption spectral profiles can give colour changes that are significant to the eye, and I think we can trust the authors to be able to distinguish 'red' from 'yellow' even at different concentrations! And the comments about different colours arising from crystal packing are not relevant to measurements in solution.

That apart, if the authors can address the comments of the first two referees the paper should be acceptable for piblication in Dalton Trans. as a communication.

Journal Name

Dynamic Article Links ►

Cite this: DOI: 10.1039/c0xx00000x

www.rsc.org/xxxxxx

ARTICLE TYPE

Stereoelectronic Control of Photophysics: Red and Yellow Axial and Equatorial Anomers of a Rhenium-Quinoline Complex

Rachel H. Platel,*[a] Michael P. Coogan[a] and James A. Platts[b]

Received (in XXX, XXX) Xth XXXXXXXXX 20XX, Accepted Xth XXXXXXXXX 20XX

DOI: 10.1039/b000000x

A novel quinoline-substituted pyrimidine ligand forms two different coloured complexes upon reaction with $Re(CO)_5Br$. These compounds display distinct photophysical properties that are dictated by their stereochemistry.

Rhenium bis(imine) complexes $[Re(CO)_3(N^N)L]$ often have interesting photophysical properties, usually emitting from ^{3}MLCT states with long luminescence lifetimes and large Stokes shifts.[1,2] Their absorption and emission properties have been widely investigated and are exploited in areas as diverse as biological imaging,[3] OLEDs,[4] photocatalysis[5] and photovoltaics.[6] Certain examples are responsive to the presence of other ions or molecules and have been used in luminescence sensing and assays.[7] These complexes all have a *fac*- geometry and, in the cases of symmetrical N^N ligands, are achiral, so to the best of our knowledge have not been used as stereochemical probes.

Complexes involving a Het^NR^Het motif (het = Py, quinoline or similar) such as dipicolyl amine have been applied in imaging involving bioconjugation to peptides through a lysine side-chain in the Single Amino Acid Chelate (SAAC) approach (Fig. 1).[8]

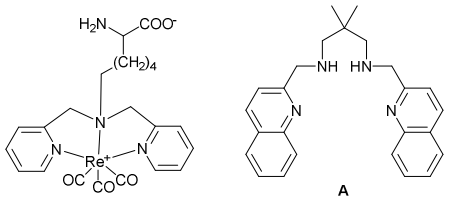

Fig. 1 Example of the SAAC approach and target ligand **A**.

These complexes show particularly rich and versatile photophysics with the dipicolyl amine complexes being UV absorbing, and visible emitting, the quinoline analogues red shifted into the visible for both transitions, and the thiazoles showing emission wavelengths which vary as a function of excitation.[9]

If the electron density in the excited state is located on one or both of the heterocycles with little or no contribution from the central NR unit, and little interaction between them, then an isolated Het^NR unit could be expected to show similar photophysics. The coordinatively unsaturated core would then allow for either further tuning of the photophysics, or interaction with ions and molecules in sensing applications. Reductive amination of heterocyclic aldehydes with diamines, gives dimeric analogues of the isolated NR^Het ~~this~~ unit (i.e. a Het^NRN^Het motif) which could form stereochemically interesting complexes with 2 or 3 coordinated nitrogen atoms, with the possibility of fluxionality between these cases.

As a preliminary investigation into this area we attempted to prepare the tethered bis(aminoquinoline) ligand **A** (Fig. 1), which, by analogy with the SAAC analogue, we anticipated should form a $Re(CO)_3$ complex with lower energy absorption and emission than the pyridine analogues.

Reaction of 2,2-dimethyl-1,3-propane diamine with 2 eq. quinoline 2-carboxaldehyde, followed by reduction with an excess of sodium borohydride gave, upon work up, a brown solid.

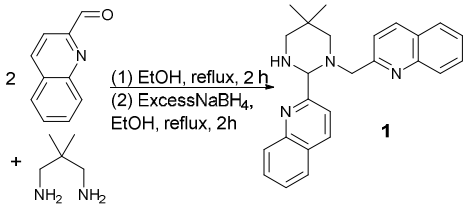

Scheme 1 Synthesis of **1**.

A ^{1}H NMR spectrum of the crude reaction mixture indicated a mixture of products was present. Recrystallization from a hot dichloromethane solution provided **1** cleanly, as a colourless, crystalline solid in 61% yield (Scheme 1). Characterization data revealed that this was not the expected bis(aminoquinoline) product, **A**, but rather, that substituted hexahydropyrimidine **1** had been formed. X-ray crystallographic analysis of a single crystal grown from a dichloromethane solution confirmed the ligand structure (Fig. 2).

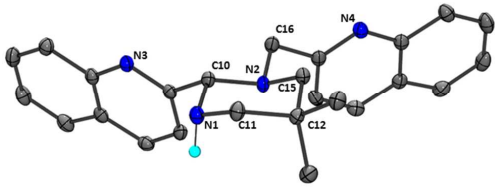

Fig. 2 Molecular Structure of **1**. Thermal ellipsoids are shown at 50% level. Non-NH hydrogens are omitted for clarity.

Formatted: Font: (Default) Times New Roman, 9 pt, Not Italic

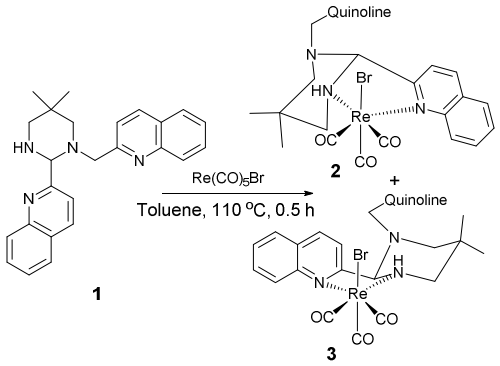

Scheme 2 Synthesis of **2** and **3**.

In the solid state structure of **1**, the pyrimidine adopts a chair conformation, with both quinoline substituents occupying equatorial positions. Non-quinoline bond lengths fall within the expected values for C–N single bonds, ranging from 1.4568(15) to 1.4868(14) Å.

The ^{1}H NMR spectrum of compound **1** suggests that this structure is maintained in solution (dynamic equilibrium is assumed, but with a vanishingly small concentration of the ring-open form). In particular, eleven aromatic signals indicate inequivalence of the quinoline moieties, a singlet at 4.49 ppm is assigned to the methine H and a 4-bond W coupling is observed between equatorial hydrogens on C11 and C16, with $^{4}J_{HH}$ of 1.6 Hz. The ligand exists as a single anomer with both quinoline groups equatorial in order to reduce the energetically disfavoured axial interactions between hydrogens and the bulky quinoline groups. We propose that **1** is formed after reduction of one of the imine groups. Nucleophilic attack by the secondary amine at the imine carbon followed by proton transfer gives the pyrimidine, **1**. The 2,2-dimethyl substituents on the diamine fragment favour cyclization through this reactivity through the Thorpe-Ingold effect.[10] Indeed, use of unsubstituted 1,3-diaminopropane as the amine in this reaction provides a ligand analogous to **A** in high yield.

The reaction between **1** and an equimolar amount of $Re(CO)_5Br$ was carried out in toluene solution at 100 °C (Scheme 2). After 30 min a pale yellow precipitate had formed. This was filtered off to leave a red solution, from which red crystalline material deposited over the course of 48 h at room temperature. ^{1}H NMR spectroscopy indicated that the yellow powder and red crystals were different species, but could both be isolated cleanly from the reaction mixture with a minimal number of manipulations.

Single crystals were grown of both the yellow powder product, **2**, and the red product, **3**, from saturated solutions of acetonitrile/toluene and toluene respectively and analysed by X-ray crystallography (Figs. 3 and 4 show the solid-state structures of **2** and **3**, respectively. We were thus able to ascertain that the overall connectivity of compounds **2** and **3** is identical. The geometry at rhenium is distorted octahedral, with the rhenium centre coordinated by the secondary amine group and the adjacent quinoline nitrogen in a *cis* arrangement. The bromide lies *cis* to both the *N* donors, leading to an overall pseudo-*fac* geometry.

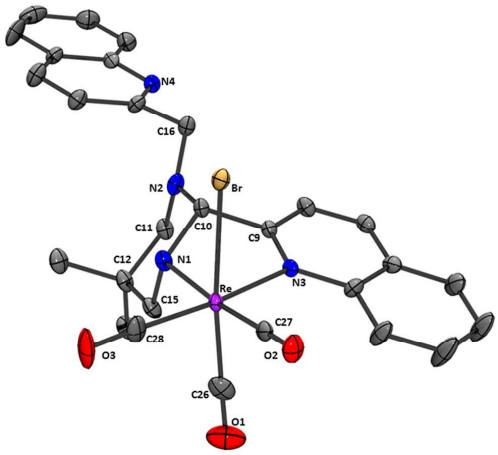

Fig. 3 Molecular structure of **2**. Thermal ellipsoids are shown at the 50% level. Hydrogen atoms are omitted for clarity.

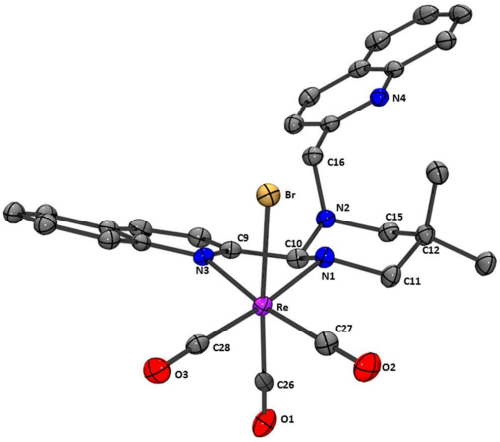

Fig. 4 Molecular structure of **3**. Thermal ellipsoids are shown at the 50% level. Hydrogen atoms are omitted for clarity.

Neither the tertiary amine group, nor the second quinoline species, participate in metal coordination in either complex. Therefore the only difference between **2** and **3** is a ring flip of the pyrimidine, where in **2** the coordinated quinoline lies axially, while in **3** it is equatorial. The uncoordinated quinoline is axial in **3** and disordered between pseudo-axial and pseudo-equatorial in **2**, however as this substituent lies on a tetrahedral nitrogen atom, in solution inversion is expected to equilibrate these conformations.

The highly unsymmetrical nature of both of these species is reflected in the complexity of their respective ^{1}H NMR spectra, with each of the methylene and quinoline hydrogens inequivalent. The fact that these two complexes have a different colour,

Journal Name

Dynamic Article Links ►

Cite this: DOI: 10.1039/c0xx00000x

www.rsc.org/xxxxxx

ARTICLE TYPE

Table 1 Spectroscopic and Photophysical data for **1** – **3**.

Compound	IR ν(C≡O) [a] cm^{-1}	UV-vis λ_{max} [b] nm (ε, M^{-1} cm^{-1})	Excitation [b] λ_{ex} /nm	Emission [b] λ_{em} /nm	Lifetime [b] /ns
1	-	273 (12560), 290 (sh, 9560), 296 (sh, 7950), 303 (7680), 310 (sh, 5860), 317 (7950)	350	420	1.3
2	2024 1927 1882	265 (sh, 13,010), 305 (9700), 320 (9060), 349 (sh, 3400), 420 (sh, reaches half height 440)	350	595	250
3	2020 1909 1871	305 (7430), 320 (5160), 335 (3520), 420 (sh, reaches half height 470)	390	595	143

[a] Neat. [b] In $CHCl_3$ solution.

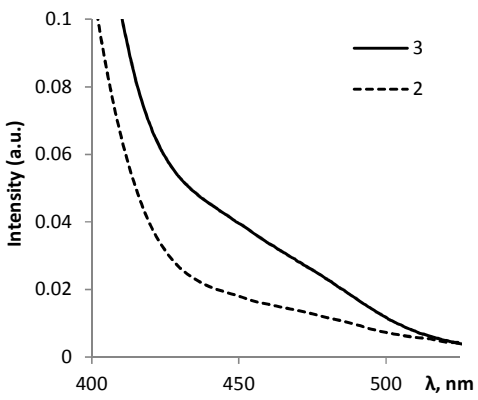

Fig. 5 Section of the UV-vis spectra of **2** and **3**.

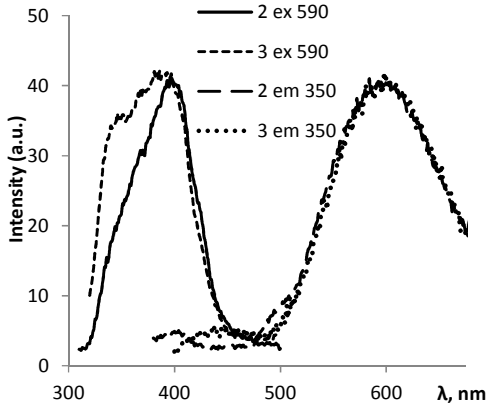

Fig. 6 Emission and Excitation Spectra for **2** and **3**.

regardless of them having identical molecular connectivities, was an entirely unexpected finding and led us to further investigate the optical properties of these species. Photophysical data are summarised in Table 1. The visible difference in appearance between **2** and **3** was reflected in the UV-vis absorption spectrum in which both **2** and **3** have bands centred at ca 350 nm which extend into the visible (*vide infra*), however there are also shoulders apparent on these tails between 420 and 520 nm, which show a large difference in intensity, with **3** having significantly more absorption in the lower energy regions (Fig. 5). These transitions were of great interest as they are broad and featureless, reminiscent of the MLCT bands associated with triplet emission in other rhenium complexes,[11] although these features are rarely associated with complexes in which a single heterocycle coordinates. Indeed, excitation into these absorption bands led to emission in the visible region, with a significant Stokes shift from the excitation maxima (350 nm, **2**, 390 nm, **3)** with both species emitting at 595 nm (Fig. 6). Whilst the excitation spectra were superficially similar, with maxima around 385 and 390 nm, the spectral shapes were clearly different, with a significant shoulder at 350 nm in **2** which is barely visible in **3**, indicating that at least 2 different transitions contribute to both excitation spectra, and that these are of significantly different ~~strengths~~ intensities in the different isomers. The lifetimes of the luminescence, 250 ns (**2**) and 143 ns (**3**), strongly suggest a triplet nature of the excited state, but the significant difference between these values was, again, unexpected for complexes with such similar connectivity.

In order to determine the nature of the electronic transitions involved in the absorption and emission processes, computational studies were undertaken which strongly supported the assignments of the observed shoulders at the UV/vis borderline as MLCT. Time-dependent DFT calculations at the B3LYP/6-31+G(d,p)_SDD level in simulated toluene solvent indicated that the lowest energy absorption bands are dominated by excitation from HOMO to LUMO, and are found at 2.91 eV / 425 nm (**3)** and 2.94 eV / 421 nm (**2**), matching the position of the tails between 420-450 nm in Fig. 5. Inspection of the form of the HOMO and LUMO in each case (Fig. 7) clearly indicate MLCT nature with the HOMOs based mainly on the $Re(CO)_3Br$ fragment, and the LUMOs concentrated in the quinoline π system. The most significant difference in orbital plots is that the

non-coordinated ring nitrogen N(2) in **2** contributes ~~significantly~~ to the HOMO, whereas it does not contribute ~~significantly~~ in **3**, indicating a contribution from distant units which appears to be under stereoelectronic control. The classic anomeric model of stereoelectronics in sugars and related systems requires an axial lone pair interacting in an antiperiplanar arrangement with orbitals at the anomeric centre,[12] and it may be significant that such an arrangement is possible in **2**, which has an axially coordinated metal-bound quinoline and an axial N-lone pair (at least in one invertomer) but would be precluded in **3.** An interaction of this sort would involve donation of the N(2) lone pair into the antibonding σ^* orbital of the C(10)–C(9) bond, ~~which is supported by~~Small differences in the relative bond lengths observed crystallographically are within error (**2**: C(10)–C(9) = 1.530(4) Å; N(2)–C(10) = 1.438(4) Å; **3**: C(10)–C(9) 1.519(4) Å, N(2)–C(10) 1.452(3) Å). However, ~~T~~the involvement of the uncoordinated N(2) lone pair in the electronic transitions is ~~further~~ supported by the loss in intensity of the absorption band observed upon protonation (see ESI).† Furthermore, simulated UV-vis spectra from the DFT calculations show that the observed low energy shoulder in **3** matches the calculated transition in which the participation of the non-coordinated ring nitrogen is implicated (see ESI).[13,14]

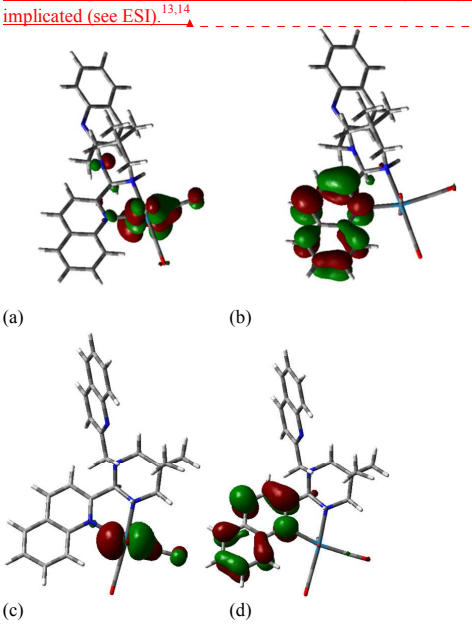

Fig. 7 DFT calculated orbital plots for: (a) the HOMO of **2**, (b) LUMO of **2,** (c) HOMO of **3**, (d) LUMO of **3**, plotted at 0.04 au isosurface

Finally, it should be noted that use of the ligands that were initially targeted (of type **A**, Fig. 1) in reactions with $Re(CO)_5Br$ give colourless products whereby the quinoline moieties do not participate in coordination and the Re centre is coordinated through the amine nitrogen atoms. In the example that was prepared (compound **4**, ESI)† the resulting complex did not exhibit fluorescence.

Conclusions

A novel pyrimidine ligand incorporating two quinoline substituents has been prepared as a single isomer in a high yielding, one-pot reaction from commercially available starting materials. This ligand forms rhenium complexes selectively as two different isomers, easily separated from each other through precipitation and recrystallization. The complexes have different colours and show different photophysical properties, which we assign as MLCT transitions under stereoelectronic control of a pseudo-anomeric effect. This effect is proposed to be a rare example of stereoelectronic control of photophysical properties, and suggests a possible platform for the design of optical probes for stereochemistry.

We thank the EPSRC UK National Crystallography Service at the University of Southampton for the collection of the crystallographic data and the EPSRC UK National Mass Spectrometry Facility for the collection of mass spectra.

Notes and references

[a] *Department of Chemistry, Lancaster University, Lancaster, LA1 1AE, UK. Tel: +44(0)1524 592557; E-mail: r.platel@lancaster.ac.uk*
[b] *School of Chemistry, Cardiff University, Main Building, Park Place, Cardiff, CF10 3AT, UK.*

† Electronic Supplementary Information (ESI) available: Full experimental, characterization details, ^1H and $^{13}C\{^1H\}$ NMR spectra, crystallographic data for **1**-**4**; additional UV-vis spectra for **2** and **3**, details of computational calculations. See DOI: 10.1039/b000000x/

1. D. J. Stufkens and A. Vlcek, Jr, *Coord. Chem. Rev.*, 1998, **177**, 127.
2. M. S. Wrighton and D. L. Morse, *J. Am. Chem. Soc.*, 1974, **96**, 998.
3. M. P. Coogan and V. Fernández-Moreira *Chem. Commun.*, 2014, **50**, 384.
4. S. Ranjan, S.-Y. Lin, K.-C. Hwang, Y. Chi, W.-L. Ching, C.-S. Liu, Y.-T. Tao, C.-H. Chien, S.-M. Peng, and G.-H. Lee, *Inorg. Chem.*, 2003, **42**, 1248.
5. P. Kurz, B. Probst, B. Spingler and R. Alberto, *Eur. J. Inorg. Chem.*, 2006, 2966.
6. F. He, Y. Zhou, S. Liu, L. Tian, H. Xu, H. Zhang, B. Yang, Q. Dong, W. Tian, Y. Ma and J. Shen, *Chem. Commun.*, 2008, 3912.
7. P.D. Beer and E.J. Hayes, *Coord. Chem. Rev.*, 2003, **240**, 167.
8. S. R. Banerjee, J. W. Babich and J. Zubieta, *Chem. Commun.*, 2005, 1784.
9. K. E. Henry, R. G. Balasingham, A. R. Vortherms, J. A. Platts, J. F. Valliant, M. P. Coogan, J. Zubieta and R. P. Doyle, *Chem. Sci.*, 2013, **4**, 2490
10. R. M. Beesley, C. K. Ingold and J. F. Thorpe *J. Chem. Soc., Trans.*, 1915, **107**, 1080.
11. L. Sacksteder, M. Lee, J. N. Demas and B. A. DeGraff *J. Am. Chem. Soc.*, 1993, **115**, 8230.
12. R. U. Lemieux, *Pure Appl. Chem.*, 1971, **25**, 527 and references therein.
13. M. Obata, A. Kitamura, A. Mori, C. Kameyama, J.A. Czaplewska, R. Tanaka, I. Kinoshita, T. Kusumoto, H. Hashimoto, M. Harada, Y. Mikata, T. Funabikig, S. Yano, *Dalton Trans.*, 2008, 3292.
14. H.C. Bertrand, S. Clède, R. Guillot, F. Lambert, C. Policar, *Inorg. Chem.* 2014, **53** 6204.

Formatted: Superscript
Formatted: N3 References
Formatted: Font: (Default) Times New Roman
Formatted: Font: (Default) Times New Roman, Italic
Formatted: Font: (Default) Times New Roman
Formatted: Font: (Default) Times New Roman
Formatted: Font: (Default) Times New Roman
Formatted: Font: (Default) Times New Roman, Italic
Formatted: Font: (Default) Times New Roman
Formatted: Font: (Default) Times New Roman

Cite this: DOI: 10.1039/c0xx00000x

www.rsc.org/xxxxxx

ARTICLE TYPE

Stereoelectronic Control of Photophysics: Red and Yellow Axial and Equatorial Anomers of a Rhenium-Quinoline Complex

Rachel H. Platel,*[a] Michael P. Coogan[a] and James A. Platts[b]

Received (in XXX, XXX) Xth XXXXXXXXX 20XX, Accepted Xth XXXXXXXXX 20XX

DOI: 10.1039/b000000x

A novel quinoline-substituted pyrimidine ligand forms two different coloured complexes upon reaction with $Re(CO)_5Br$. These compounds display distinct photophysical properties that are dictated by their stereochemistry.

Rhenium bis(imine) complexes $[Re(CO)_3(N^N)L]$ often have interesting photophysical properties, usually emitting from ^{3}MLCT states with long luminescence lifetimes and large Stokes shifts.[1,2] Their absorption and emission properties have been widely investigated and are exploited in areas as diverse as biological imaging,[3] OLEDs,[4] photocatalysis[5] and photovoltaics.[6] Certain examples are responsive to the presence of other ions or molecules and have been used in luminescence sensing and assays.[7] These complexes all have a *fac*- geometry and, in the cases of symmetrical N^N ligands, are achiral, so to the best of our knowledge have not been used as stereochemical probes.

Complexes involving a Het^NR^Het motif (het = Py, quinoline or similar) such as dipicolyl amine have been applied in imaging involving bioconjugation to peptides through a lysine side-chain in the Single Amino Acid Chelate (SAAC) approach (Fig. 1).[8]

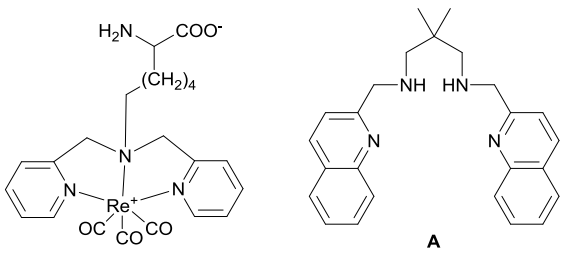

Fig. 1 Example of the SAAC approach and target ligand **A**.

These complexes show particularly rich and versatile photophysics with the dipicolyl amine complexes being UV absorbing, and visible emitting, the quinoline analogues red shifted into the visible for both transitions, and the thiazoles showing emission wavelengths which vary as a function of excitation.[9]

If the electron density in the excited state is located on one or both of the heterocycles with little or no contribution from the central NR unit, and little interaction between them, then an isolated Het^NR unit could be expected to show similar photophysics. The coordinatively unsaturated core would then allow for either further tuning of the photophysics, or interaction with ions and molecules in sensing applications. Reductive amination of heterocyclic aldehydes with diamines, gives dimeric analogues of the isolated NR^Het unit (i.e. a Het^NRN^Het motif) which could form stereochemically interesting complexes with 2 or 3 coordinated nitrogen atoms, with the possibility of fluxionality between these cases.

As a preliminary investigation into this area we attempted to prepare the tethered bis(aminoquinoline) ligand **A** (Fig. 1), which, by analogy with the SAAC analogue, we anticipated should form a $Re(CO)_3$ complex with lower energy absorption and emission than the pyridine analogues.

Reaction of 2,2-dimethyl-1,3-propane diamine with 2 eq. quinoline 2-carboxaldehyde, followed by reduction with an excess of sodium borohydride gave, upon work up, a brown solid.

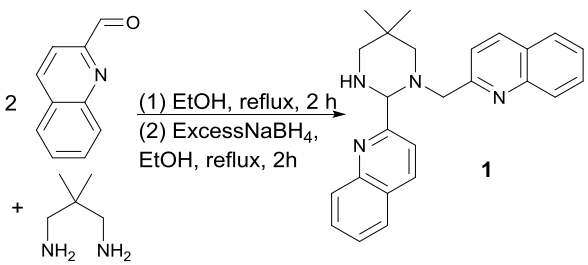

Scheme 1 Synthesis of **1**.

A ^{1}H NMR spectrum of the crude reaction mixture indicated a mixture of products was present. Recrystallization from a hot dichloromethane solution provided **1** cleanly, as a colourless, crystalline solid in 61% yield (Scheme 1). Characterization data revealed that this was not the expected bis(aminoquinoline) product, **A**, but rather, that substituted hexahydropyrimidine **1** had been formed. X-ray crystallographic analysis of a single crystal grown from a dichloromethane solution confirmed the ligand structure (Fig. 2).

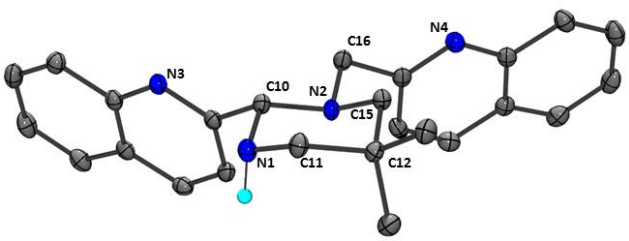

Fig. 2 Molecular Structure of **1**. Thermal ellipsoids are shown at 50% level. Non-NH hydrogens are omitted for clarity.

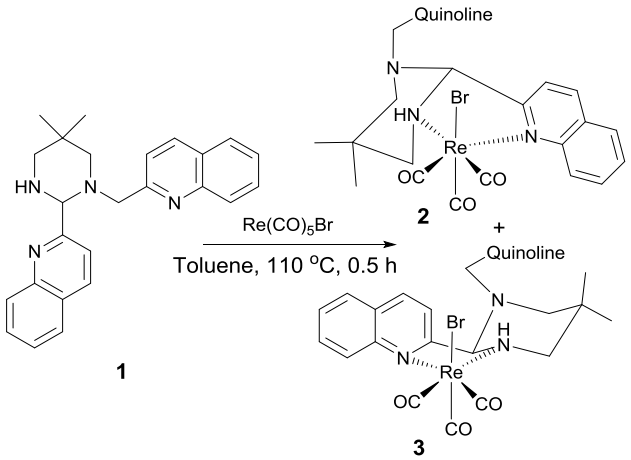

Scheme 2 Synthesis of **2** and **3**.

In the solid state structure of **1**, the pyrimidine adopts a chair conformation, with both quinoline substituents occupying equatorial positions. Non-quinoline bond lengths fall within the expected values for C–N single bonds, ranging from 1.4568(15) to 1.4868(14) Å.

The ^{1}H NMR spectrum of compound **1** suggests that this structure is maintained in solution (dynamic equilibrium is assumed, but with a vanishingly small concentration of the ring-open form). In particular, eleven aromatic signals indicate inequivalence of the quinoline moieties, a singlet at 4.49 ppm is assigned to the methine H and a 4-bond W coupling is observed between equatorial hydrogens on C11 and C16, with $^{4}J_{HH}$ of 1.6 Hz. The ligand exists as a single anomer with both quinoline groups equatorial in order to reduce the energetically disfavoured axial interactions between hydrogens and the bulky quinoline groups. We propose that **1** is formed after reduction of one of the imine groups. Nucleophilic attack by the secondary amine at the imine carbon followed by proton transfer gives the pyrimidine, **1**. The 2,2-dimethyl substituents on the diamine fragment favour cyclization through this reactivity through the Thorpe-Ingold effect.[10] Indeed, use of unsubstituted 1,3-diaminopropane as the amine in this reaction provides a ligand analogous to **A** in high yield.

The reaction between **1** and an equimolar amount of $Re(CO)_5Br$ was carried out in toluene solution at 100 °C (Scheme 2). After 30 min a pale yellow precipitate had formed. This was filtered off to leave a red solution, from which red crystalline material deposited over the course of 48 h at room temperature. ^{1}H NMR spectroscopy indicated that the yellow powder and red crystals were different species, but could both be isolated cleanly from the reaction mixture with a minimal number of manipulations.

Single crystals were grown of both the yellow powder product, **2**, and the red product, **3**, from saturated solutions of acetonitrile/toluene and toluene respectively and analysed by X-ray crystallography (Figs. 3 and 4 show the solid-state structures of **2** and **3**, respectively. We were thus able to ascertain that the overall connectivity of compounds **2** and **3** is identical. The geometry at rhenium is distorted octahedral, with the rhenium centre coordinated by the secondary amine group and the adjacent quinoline nitrogen in a *cis* arrangement. The bromide lies *cis* to both the *N* donors, leading to an overall pseudo-*fac* geometry.

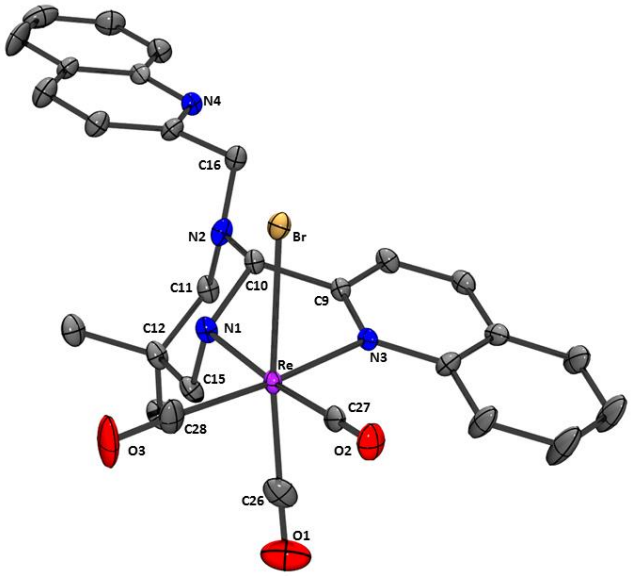

Fig. 3 Molecular structure of **2**. Thermal ellipsoids are shown at the 50% level. Hydrogen atoms are omitted for clarity.

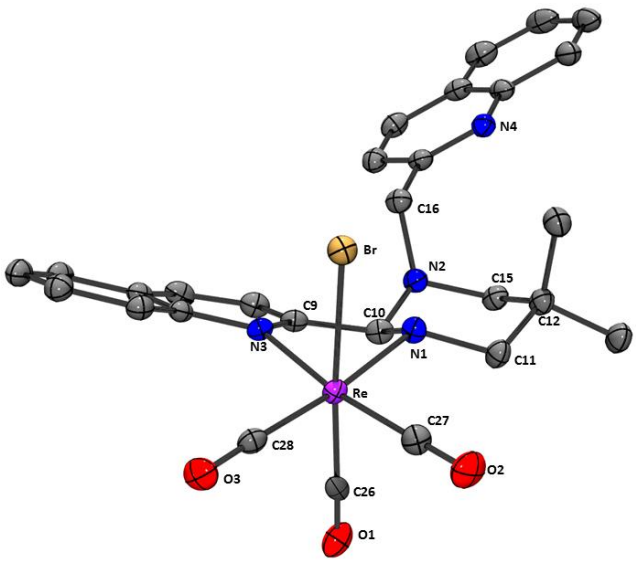

Fig. 4 Molecular structure of **3**. Thermal ellipsoids are shown at the 50% level. Hydrogen atoms are omitted for clarity.

Neither the tertiary amine group, nor the second quinoline species, participate in metal coordination in either complex. Therefore the only difference between **2** and **3** is a ring flip of the pyrimidine, where in **2** the coordinated quinoline lies axially, while in **3** it is equatorial. The uncoordinated quinoline is axial in **3** and disordered between pseudo-axial and pseudo-equatorial in **2**, however as this substituent lies on a tetrahedral nitrogen atom, in solution inversion is expected to equilibrate these conformations.

The highly unsymmetrical nature of both of these species is reflected in the complexity of their respective ^{1}H NMR spectra, with each of the methylene and quinoline hydrogens inequivalent. The fact that these two complexes have a different colour,

Cite this: DOI: 10.1039/c0xx00000x

www.rsc.org/xxxxxx

ARTICLE TYPE

Table 1 Spectroscopic and Photophysical data for **1** – **3**.

Compound	IR υ(C≡O) [a] cm^{-1}	UV-vis λ_{max} [b] nm (ε, M^{-1} cm^{-1})	Excitation [b] λ_{ex} /nm	Emission [b] λ_{em} /nm	Lifetime [b] /ns
1	-	273 (12560), 290 (sh, 9560), 296 (sh, 7950), 303 (7680), 310 (sh, 5860), 317 (7950)	350	420	1.3
2	2024 1927 1882	265 (sh, 13,010), 305 (9700), 320 (9060), 349 (sh, 3400), 420 (sh, reaches half height 440)	350	595	250
3	2020 1909 1871	305 (7430), 320 (5160), 335 (3520), 420 (sh, reaches half height 470)	390	595	143

[a] Neat. [b] In $CHCl_3$ solution.

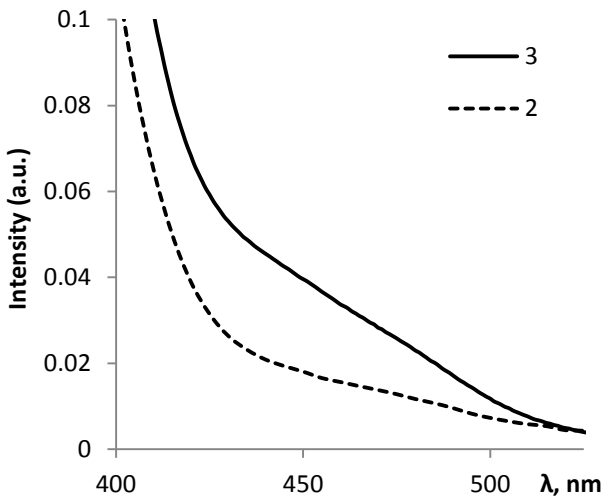

Fig. 5 Section of the UV-vis spectra of **2** and **3**.

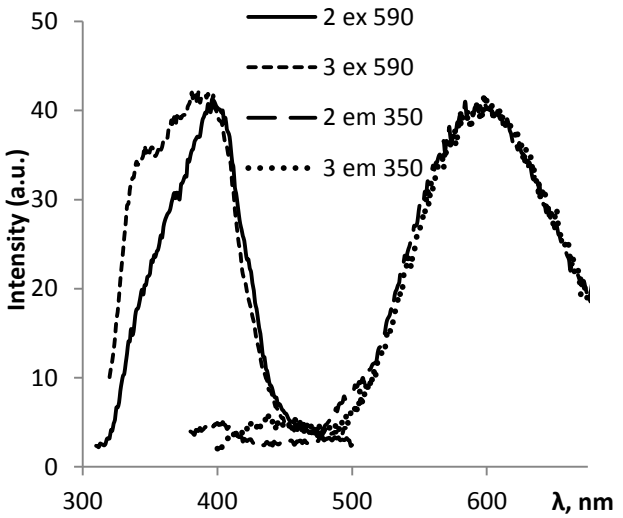

Fig. 6 Emission and Excitation Spectra for **2** and **3**.

regardless of them having identical molecular connectivities, was an entirely unexpected finding and led us to further investigate the optical properties of these species. Photophysical data are summarised in Table 1. The visible difference in appearance between **2** and **3** was reflected in the UV-vis absorption spectrum in which both **2** and **3** have bands centred at ca 350 nm which extend into the visible (*vide infra*), however there are also shoulders apparent on these tails between 420 and 520 nm, which show a large difference in intensity, with **3** having significantly more absorption in the lower energy regions (Fig. 5). These transitions were of great interest as they are broad and featureless, reminiscent of the MLCT bands associated with triplet emission in other rhenium complexes,[11] although these features are rarely associated with complexes in which a single heterocycle coordinates. Indeed, excitation into these absorption bands led to emission in the visible region, with a significant Stokes shift from the excitation maxima (350 nm, **2**, 390 nm, **3)** with both species emitting at 595 nm (Fig. 6). Whilst the excitation spectra were superficially similar, with maxima around 385 and 390 nm, the spectral shapes were clearly different, with a significant shoulder at 350 nm in **2** which is barely visible in **3**, indicating that at least 2 different transitions contribute to both excitation spectra, and that these are of significantly different intensities in the different isomers. The lifetimes of the luminescence, 250 ns (**2**) and 143 ns (**3**), strongly suggest a triplet nature of the excited state, but the significant difference between these values was, again, unexpected for complexes with such similar connectivity.

In order to determine the nature of the electronic transitions involved in the absorption and emission processes, computational studies were undertaken which strongly supported the assignments of the observed shoulders at the UV/vis borderline as MLCT. Time-dependent DFT calculations at the B3LYP/6-31+G(d,p)_SDD level in simulated toluene solvent indicated that the lowest energy absorption bands are dominated by excitation from HOMO to LUMO, and are found at 2.91 eV / 425 nm (**3)** and 2.94 eV / 421 nm (**2**), matching the position of the tails between 420-450 nm in Fig. 5. Inspection of the form of the HOMO and LUMO in each case (Fig. 7) clearly indicate MLCT nature with the HOMOs based mainly on the $Re(CO)_3Br$ fragment, and the LUMOs concentrated in the quinoline π system. The most significant difference in orbital plots is that the non-coordinated ring nitrogen N(2) in **2** contributes to the

HOMO, whereas it does not contribute in **3**, indicating a contribution from distant units which appears to be under stereoelectronic control. The classic anomeric model of stereoelectronics in sugars and related systems requires an axial lone pair interacting in an antiperiplanar arrangement with orbitals at the anomeric centre,[12] and it may be significant that such an arrangement is possible in **2**, which has an axially coordinated metal-bound quinoline and an axial N-lone pair (at least in one invertomer) but would be precluded in **3.** An interaction of this sort would involve donation of the N(2) lone pair into the antibonding σ^* orbital of the C(10)–C(9) bond. Small differences in the relative bond lengths observed crystallographically are within error (**2**: C(10)–C(9) = 1.530(4) Å; N(2)–C(10) = 1.438(4) Å; **3**: C(10)–C(9) 1.519(4) Å, N(2)–C(10) 1.452(3) Å). However, the involvement of the uncoordinated N(2) lone pair in the electronic transitions is supported by the loss in intensity of the absorption band observed upon protonation (see ESI).† Furthermore, simulated UV-vis spectra from the DFT calculations show that the observed low energy shoulder in **3** matches the calculated transition in which the participation of the non-coordinated ring nitrogen is implicated (see ESI).[13,14]

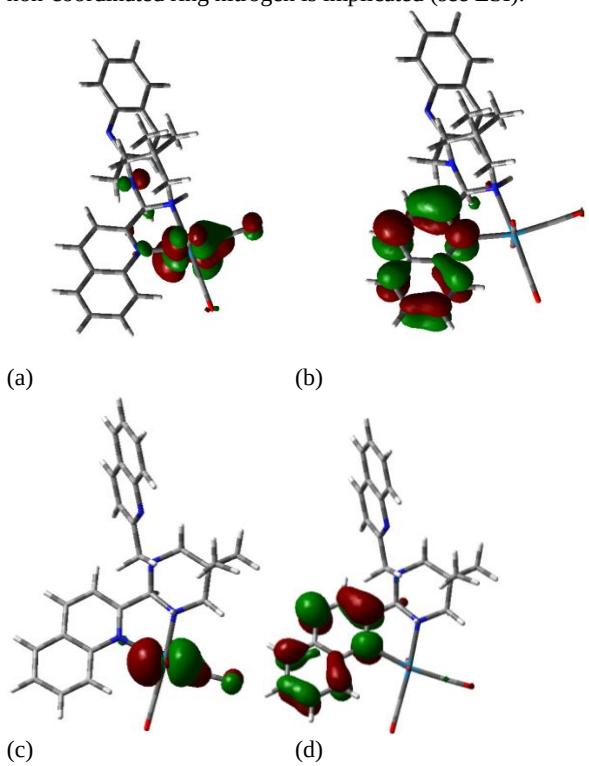

Fig. 7 DFT calculated orbital plots for: (a) the HOMO of **2**, (b) LUMO of **2,** (c) HOMO of **3**, (d) LUMO of **3**, plotted at 0.04 au isosurface

Finally, it should be noted that use of the ligands that were initially targeted (of type **A**, Fig. 1) in reactions with $Re(CO)_5Br$ give colourless products whereby the quinoline moieties do not participate in coordination and the Re centre is coordinated through the amine nitrogen atoms. In the example that was prepared (compound **4**, ESI)† the resulting complex did not exhibit fluorescence.

Conclusions

A novel pyrimidine ligand incorporating two quinoline substituents has been prepared as a single isomer in a high yielding, one-pot reaction from commercially available starting materials. This ligand forms rhenium complexes selectively as two different isomers, easily separated from each other through precipitation and recrystallization. The complexes have different colours and show different photophysical properties, which we assign as MLCT transitions under stereoelectronic control of a pseudo-anomeric effect. This effect is proposed to be a rare example of stereoelectronic control of photophysical properties, and suggests a possible platform for the design of optical probes for stereochemistry.

We thank the EPSRC UK National Crystallography Service at the University of Southampton for the collection of the crystallographic data and the EPSRC UK National Mass Spectrometry Facility for the collection of mass spectra.

Notes and references

[a] *Department of Chemistry, Lancaster University, Lancaster, LA1 1AE, UK. Tel: +44(0)1524 592557; E-mail: r.platel@lancaster.ac.uk*
[b] *School of Chemistry, Cardiff University, Main Building, Park Place, Cardiff, CF10 3AT, UK.*

† Electronic Supplementary Information (ESI) available: Full experimental, characterization details, ^1H and $^{13}C\{^1H\}$ NMR spectra, crystallographic data for **1**-**4**; additional UV-vis spectra for **2** and **3**, details of computational calculations. See DOI: 10.1039/b000000x/

1. D. J. Stufkens and A. Vlcek, Jr, *Coord. Chem. Rev.*, 1998, **177**, 127.
2. M. S. Wrighton and D. L. Morse, *J. Am. Chem. Soc.*, 1974, **96**, 998.
3. M. P. Coogan and V. Fernández-Moreira *Chem. Commun.*, 2014, **50**, 384.
4. S. Ranjan, S.-Y. Lin, K.-C. Hwang, Y. Chi, W.-L. Ching, C.-S. Liu, Y.-T. Tao, C.-H. Chien, S.-M. Peng, and G.-H. Lee, *Inorg. Chem.*, 2003, **42**, 1248.
5. P. Kurz, B. Probst, B. Spingler and R. Alberto, *Eur. J. Inorg. Chem.*, 2006, 2966.
6. F. He, Y. Zhou, S. Liu, L. Tian, H. Xu, H. Zhang, B. Yang, Q. Dong, W. Tian, Y. Ma and J. Shen, *Chem. Commun.*, 2008, 3912.
7. P.D. Beer and E.J. Hayes, *Coord. Chem. Rev.*, 2003, **240**, 167.
8. S. R. Banerjee, J. W. Babich and J. Zubieta, *Chem. Commun.*, 2005, 1784.
9. K. E. Henry, R. G. Balasingham, A. R. Vortherms, J. A. Platts, J. F. Valliant, M. P. Coogan, J. Zubieta and R. P. Doyle, *Chem. Sci.*, 2013, **4**, 2490
10. R. M. Beesley, C. K. Ingold and J. F. Thorpe *J. Chem. Soc., Trans.*, 1915, **107**, 1080.
11. L. Sacksteder, M. Lee, J. N. Demas and B. A. DeGraff *J. Am. Chem. Soc.*, 1993, **115**, 8230.
12. R. U. Lemieux, *Pure Appl. Chem.*, 1971, **25**, 527 and references therein.
13. M. Obata, A. Kitamura, A. Mori, C. Kameyama, J.A. Czaplewska, R. Tanaka, I. Kinoshita, T. Kusumoto, H. Hashimoto, M. Harada, Y. Mikata, T. Funabikig, S. Yano, *Dalton Trans.* 2008, 3292.
14. H.C. Bertrand, S. Clède, R. Guillot, F. Lambert, C. Policar, *Inorg. Chem.* 2014, **53** 6204.

Stereoelectronic Control of Photophysics: Red and Yellow Axial and Equatorial Anomers of a Rhenium-Quinoline Complex

Rachel H. Platel,[a] Michael P. Coogan[a] and James A. Platts[b]*

[a] Department of Chemistry, Lancaster University, Lancaster, LA1 1AE, UK. Tel: +44(0)1524 592557; E-mail: r.platel@lancaster.ac.uk

[b] School of Chemistry, Cardiff University, Main Building, Park Place, Cardiff, CF10 3AT, UK.

Electronic Supplementary Information

Experimental Details……...…….2
Synthesis of **1**……...……...….2
Synthesis of **2**……...……...…….3
Synthesis of **3**…….....…….3
Synthesis of **4**……...……....…….4
UV-vis Spectra of **2** and **3**……...…….5
Decay Plots for Lifetime Calculations of **2** and **3**……6
Simulated UV-vis Spectra of **2** and **3**……...7
Computational Details……...……...…….8
Crystallographic Data for **1** – **4**……...…….9
Molecular Structure of **4**……..…...…...….10
References……...……...……10
^{1}H and ^{13}C{^{1}H} NMR spectra of **1** – **4**……...11

General Considerations

Synthesis

All starting materials, reagents and solvents were purchased from commercial suppliers and used as supplied unless otherwise stated. $Re(CO)_5Br$[1] and *N,N'*-bis(2-quinolinylmethyl)-1,2-ethylenediamine[2] were prepared according to literature methods.

Measurements

^{1}H-NMR and ^{13}C-NMR spectra were recorded at 400 and 100 MHz, respectively, on a Bruker Avance III 400 and referenced to residual solvent peaks. Chemical shifts are reported in ppm, and coupling constants in Hz. IR spectra were recorded on an Agilent Technologies Cary 630 FTIR Spectrometer as solids and are reported in wavenumbers (cm^{-1}). UV-vis spectra were recorded on an Agilent Technologies Cary 60. Steady state emission and excitation spectra were recorded on an Agilent Technologies Cary Eclipse. Time-resolved spectra were recorded on a PicoQuant FluoTime 300 exciting with an LDH-P-C-375 and decays were analysed with the program FluoFit. Melting points are uncorrected. Mass spectra were recorded at the EPSRC National Mass Spectrometry Service Centre in Swansea on a Thermo Scientific LTQ Orbitrap XL. Elemental analyses were measured by Mr Stephen Boyer at London Metropolitan University.

Synthesis of compound **1**

Quinoline 2-carboxaldehyde (3.14 g, 20 mmol) was added, in portions, to a stirred solution of 2,2-dimethyl-1,3-propane diamine (1.24 mL, 10 mmol) in ethanol (60 mL). The resulting orange/brown solution was heated at reflux for 3 h. After allowing the solution to cool to room temperature, sodium borohydride (1 x 1 g pellet, 26.5 mmol), was added with stirring, followed by more ethanol (40 mL). The reaction mixture was heated at reflux for a futher 2 h before allowing to cool to room temperature. Water (50 mL) was added slowly to the reaction mixture, which was then extracted with dichloromethane (3 x 20 mL). The combined organic extracts were washed with brine (20 mL), dried ($MgSO_4$) and the solvents removed to leave a brown residue. Recrystallization from the minimum volume of hot dichloromethane gave the title compound as a colourless crystalline solid (2.34 g, 61%). ^{1}H NMR (400 MHz, $CDCl_3$) δ ppm: 8.17 (1H, d, $^3J_{HH}$ = 8.4 Hz, ArH^4), 8.15 (1H, m, ArH^8), 8.09 (1H, d, $^3J_{HH}$ = 8.4 Hz, ArH^4), 7.96 (1H, m, ArH^8), 7.84 (1H, d, $^3J_{HH}$ = 8.4 Hz, ArH^3), 7.77 (2H, m, ArH^5), 7.75 (1H, d, $^3J_{HH}$ = 8.4 Hz, ArH^3), 7.71 (1H, ddd, $^3J_{HH}$ = 8.6 Hz, $^3J_{HH}$ = 6.9 Hz, $^4J_{HH}$ = 1.6 Hz, ArH^7), 7.65 (1H, ddd, $^3J_{HH}$ = 8.6 Hz, $^3J_{HH}$ = 6.9 Hz, $^4J_{HH}$ = 1.6 Hz, ArH^7), 7.52 (1H, ddd, $^3J_{HH}$ = 8.6 Hz, $^3J_{HH}$ = 6.9 Hz, $^4J_{HH}$ = 1.6 Hz, ArH^6), 7.48 (1H, ddd, $^3J_{HH}$ = 8.6 Hz, $^3J_{HH}$ = 6.9 Hz, $^4J_{HH}$ = 1.6 Hz, ArH^6), 4.49 (1H, s, CH), 3.80 (1H, d, $^2J_{HH}$ = 14.6 Hz, CH_2), 3.44 (1H, d, $^2J_{HH}$ = 14.6 Hz, CH_2), 2.81 (1H, dd, $^2J_{HH}$ = 13.2 Hz, $^4J_{HH}$ = 2.0 Hz, CH_2), 2.71 (1H, d, $^2J_{HH}$ = 13.2 Hz, CH_2), 2.65 (1H, dd, $^2J_{HH}$ = 11.6 Hz, $^4J_{HH}$ = 2.0 Hz, CH_2), 2.26 (1H, d, $^2J_{HH}$ = 11.6 Hz, CH_2), 1.99 (1H, br s, NH), 1.31 (3H,

s, CH_3), 0.82 (3H, s, CH_3); ^{13}C{^{1}H} NMR (100 MHz, $CDCl_3$) δ ppm: 161.0 (Ar*C*), 160.3 (Ar*C*), 147.9 (Ar*C*), 147.4 (Ar*C*), 137.1 (Ar*C*H), 136.2 (Ar*C*H), 129.5 (2 x Ar*C*H), 129.2 (Ar*C*H), 128.8 (Ar*C*H), 128.0 (Ar*C*), 127.45 (Ar*C*H), 127.43 (Ar*C*H), 127.3 (Ar*C*), 126.5 (Ar*C*H), 125.9 (Ar*C*H), 120.5 (Ar*C*H), 119.4 (Ar*C*H), 82.7 (*C*H), 64.5 (*C*H_2), 60.4 (*C*H_2), 57.2 (*C*H_2), 30.9 (*C*(CH_3)$_2$), 26.2 (*C*H_3), 23.7 (*C*H_3); MS, *m/z* (ES): 383 $[M]^+$; IR, ν cm^{-1}: 3293 (w N–H stretch), 3057 (w), 2959(w), 2805 (w), 1600, 1500, 1485, 1472, 1424, 1135, 1084; UV-Vis ($CHCl_3$, λ_{max} nm (ε, M^{-1} cm^{-1})): 273 (12560), 290 (sh, 9560), 296 (sh, 7950), 303 (7680), 310 (sh, 5860), 317 (7950); Anal. Calcd for $C_{25}H_{26}N_4$: C, 78.50; H, 6.85; N, 14.65 %. Found: C, 78.34, H, 6.98, N, 14.53 %.

Synthesis of Rhenium Compounds **2** and **3**

$Re(CO)_5Br$ (0.128 g, 0.316 mmol) was heated to 100 °C in toluene (10 mL) with stirring. When the solids had dissolved, **1** (0.121 g, 0.316 mmol) was added as a solid in one portion. The reaction mixture was left to stir at 100 °C for 20 min, during which time a yellow precipitate formed. Hot filtration of the reaction mixture afforded **2** (0.045 g, 19 %) as a yellow powder. Upon cooling, red crystals formed in the filtrate. These were recovered by filtration to give **3** (0.151 g, 65%) as a red crystalline solid.

Compound **2**: ^{1}H NMR (400 MHz, $CDCl_3$) δ ppm: 8.87 (1H, d, $^3J_{HH}$ = 8.8 Hz, Ar*H*^{8}), 8.38 (1H, d, $^3J_{HH}$ = 8.4 Hz, Ar*H*^{4}), 8.19 (1H, d, $^3J_{HH}$ = 8.4 Hz, Ar*H*^{4}), 8.17 (1H, d, $^3J_{HH}$ = 7.6 Hz, Ar*H*^{5}), 8.10 (1H, d, $^3J_{HH}$ = 8.4 Hz, Ar*H*^{3}), 7.94 (2H, m, Ar*H*^{7,8}), 7.82 (1H, d, $^3J_{HH}$ = 8.0 Hz, Ar*H*^{5}), 7.72 (2H, m, Ar*H*^{5,6}), 7.55 (1H, m, Ar*H*^{7}), 7.49 (1H, d, $^3J_{HH}$ = 8.4 Hz, Ar*H*^{3}), 7.01 (1H, m, C*H*), 5.10 (1H, br d, $^3J_{HH}$ = 13.0 Hz, N*H*), 4.74 (1H, d, $^2J_{HH}$ = 15.2 Hz, CH_2), 4.68 (1H, d, $^2J_{HH}$ = 15.2 Hz, CH_2), 3.27 (1H, d, $^2J_{HH}$ = 13.7 Hz, CH_2), 2.91 (1H, d, $^2J_{HH}$ = 14.4 Hz, CH_2), 2.87 (1H, d, $^2J_{HH}$ = 14.4 Hz, CH_2), 2.67 (1H, dd, $^2J_{HH}$ = 13.7 Hz, $^3J_{HH}$ = 13.0 Hz, CH_2), 1.27 (3H, s, CH_3), 0.69 (3H, s, CH_3); ^{13}C{^{1}H} NMR (100 MHz, $CDCl_3$) δ ppm: 195.2 (*C*≡O), 195.1 (*C*≡O), 191.4 (*C*≡O), 161.5 (Ar*C*), 158.6 (Ar*C*), 148.0 (Ar*C*), 147.6 (Ar*C*), 140.5 (Ar*C*H), 137.2 (Ar*C*H), 132.3 (Ar*C*H), 130.4 (Ar*C*H), 130.0 (Ar*C*H), 129.2 (Ar*C*H), 128.7 (Ar*C*H), 128.7 (Ar*C*), 128.15 (Ar*C*H), 127.6 (Ar*C*H), 127.4 (Ar*C*), 126.7 (Ar*C*H), 121.7 (Ar*C*H), 120.5 (Ar*C*H), 79.3 (*C*H), 63.9 (*C*H_2), 62.8 (*C*H_2), 56.9 (*C*H_2), 31.4(*C*(CH_3)$_2$), 26.1 (*C*H_3), 23.6 (*C*H_3); MS, *m/z* (ES): 747 (45%) $[M + NH_4]^+$, 733 (65%) $[M]^+$, 689 (90%) $[M - CO]^+$, 653 (100 %) $[M - Br]^+$; IR, ν cm^{-1}: 3175 (m, N–H stretch), 2951 (w), 2925 (w), 2851 (w), 2024 (s, C≡O), 1927 (s, C≡O), 1882 (s, C≡O), 1603, 1510, 1465, 1432, 1372, 1149, 1097; UV-Vis ($CHCl_3$, λ_{max} nm (ε, M^{-1} cm^{-1})): 265 (sh, 13,010), 305 (9700), 320 (9060), 349 (sh, 3400), 449 (sh, 190), 500 (100); Anal. Calcd for $C_{28}H_{29}BrN_4O_3Re$: C, 45.71; H, 3.97; N, 7.62 %. Found: C, 45.64, H, 3.92, N, 7.56 %.

Compound **3**: ^{1}H NMR (400 MHz, $CDCl_3$) δ ppm: 9.01 (1H, d, $^3J_{HH}$ = 8.8 Hz, Ar*H*^{8}), 8.24 (1H, d, $^3J_{HH}$ = 8.4 Hz, Ar*H*^{4}), 8.23 (1H, d, $^3J_{HH}$ = 8.4 Hz, Ar*H*^{4}), 8.05 (1H, d, $^3J_{HH}$ = 8.0 Hz, Ar*H*^{8}), 7.94 (1H, ddd, $^3J_{HH}$ = 7.8 Hz, $^3J_{HH}$ = 7.6 Hz, $^4J_{HH}$ = 1.6 Hz, Ar*H*^{7}), 7.88 (1H, m, Ar*H*^{5}), 7.83 (1H, dd, $^3J_{HH}$ = 8.0

Hz, $^4J_{HH}$ = 1.2 Hz, Ar*H*^{5}), 7.75 (1H, m, Ar*H*^{7}), 7.74 (1H, d, $^3J_{HH}$ = 8.4 Hz, Ar*H*^{3}), 7.69 (1H, m, Ar*H*^{6}), 7.61 (1H, d, $^3J_{HH}$ = 8.4 Hz, Ar*H*^{3}), 7.59 (1H, m, Ar*H*^{6}), 5.55 (1H, d, $^3J_{HH}$ = 10.1 Hz, C*H*), 4.49 (1H, m, N*H*), 4.42 (1H, d, $^2J_{HH}$ = 15.2 Hz, CH_2), 3.94 (1H, d, $^2J_{HH}$ = 15.2 Hz, CH_2), 3.75 (1H, dm, $^2J_{HH}$ = 13.2 Hz, CH_2), 3.40 (1H, dd, $^2J_{HH}$ = 13.2 Hz, $^3J_{HH}$ = 13.0 Hz, CH_2), 3.29 (1H, d, $^2J_{HH}$ = 14.4 Hz, CH_2), 3.13 (1H, dd, $^2J_{HH}$ = 14.4 Hz, $^4J_{HH}$ = 2.0 Hz, CH_2), 1.47 (3H, s, CH_3), 0.96 (3H, s, CH_3); ^{13}C{^{1}H} NMR (100 MHz, $CDCl_3$) δ ppm: 195.6 (*C*≡O), 195.2 (*C*≡O), 190.4 (*C*≡O), 159.9 (Ar*C*), 158.0 (Ar*C*), 147.9 (Ar*C*), 147.6 (Ar*C*), 140.4 (Ar*C*H), 137.1 (Ar*C*H), 132.2 (Ar*C*H), 130.9 (Ar*C*H), 129.9 (Ar*C*H), 129.1 (Ar*C*H), 128.8 (Ar*C*), 128.6 (Ar*C*H), 128.18 (Ar*C*H), 127.6 (Ar*C*H), 127.3 (Ar*C*), 126.6 (Ar*C*H), 119.7 (Ar*C*H), 119.5 (Ar*C*H), 87.1 (*C*H), 66.2 (*C*H_2), 59.8 (*C*H_2), 53.6 (*C*H_2), 31.3 (*C*$(CH_3)_2$), 27.5 (*C*H_3), 27.0 (*C*H_3); MS, *m/z* (ES): 747 (15%) $[M + NH_4]^+$, 733 (100%) $[M]^+$, 689 (15%) $[M - CO]^+$, 653 (30%) $[M - Br]^+$, 383 (50%) $[M - Br - 3(CO)]^+$; IR, *v* cm^{-1}: 3197 (m, N–H stretch), 2959 (w), 2928 (w), 2910 (w), 2020 (s, C≡O), 1909 (s, C≡O), 1871 (s, C≡O), 1599, 1510, 1462, 1432, 1376, 1302, 1227, 1153, 1115; UV-Vis ($CHCl_3$, λ_{max} nm (ε, M^{-1} cm^{-1})): 305 (7434), 320 (5155), 335 (3520), 449 (sh, 262), 494 (149), 635 (69); Anal. Calcd for $C_{28}H_{29}BrN_4O_3Re.C_7H_8$: C, 50.78; H, 4.51; N, 6.77 %. Found: C, 50.66, H, 4.47, N, 6.67 %.

Synthesis of Compound **4**

$Re(CO)_5Br$ (0.122 g, 0.30 mmol) was heated to 100 °C in toluene (8 mL) with stirring. When the solids had dissolved, *N,N'*-bis(2-quinolinylmethyl)-1,2-ethylenediamine (0.103 g, 0.30 mmol) was added in toluene (2 mL), *via* a pipette. The reaction mixture was left to stir at 100 °C for 30 min, during which time the reaction mixture turned beige and a pale yellow precipitate formed. Hot filtration of the reaction mixture afforded **4** (0.084 g, 39 %) as an off white powder. The filtrate was also identified as **4**. Crystals suitable for single crystal X-ray diffraction were grown by slow evaporation from a chloroform solution. ^{1}H NMR (400 MHz, $CDCl_3$) δ ppm: 8.22 (2H, d, $^3J_{HH}$ = 8.0 Hz, Ar*H*), 8.14 (2H, d, $^3J_{HH}$ = 8.0 Hz, Ar*H*), 7.84 (2H, d, $^3J_{HH}$ = 8.0 Hz, Ar*H*), 7.77 (2H, m, Ar*H*), 7.59 (2H, m, Ar*H*), 7.35 (2H, d, $^3J_{HH}$ = 8.0 Hz, Ar*H*), 5.26 (2H, m, N*H*), 4.81 (2H, m, CH_2), 4.77 (2H, m, CH_2), 3.62 (2H, m, CH_2), 2.89 (2H, m, CH_2); ^{13}C{^{1}H} NMR (100 MHz, $CDCl_3$) δ ppm: 194.3 (C≡O), 193.8 (C≡O), 192.5 (C≡O), 154.7 (Ar*C*), 147.6 (Ar*C*), 137.5 (Ar*C*), 130.2 (Ar*C*), 129.0 (Ar*C*), 128.2 (Ar*C*), 127.6 (Ar*C*), 127.0 (Ar*C*), 119.8 (Ar*C*), 62.3 (*C*H_2), 51.7 (*C*H_2); HRMS, *m/z* (ES): Calcd for $C_{25}H_{23}BrN_4O_3Re$, 693.0489 $[M + H]^+$; Found, 693.0483.

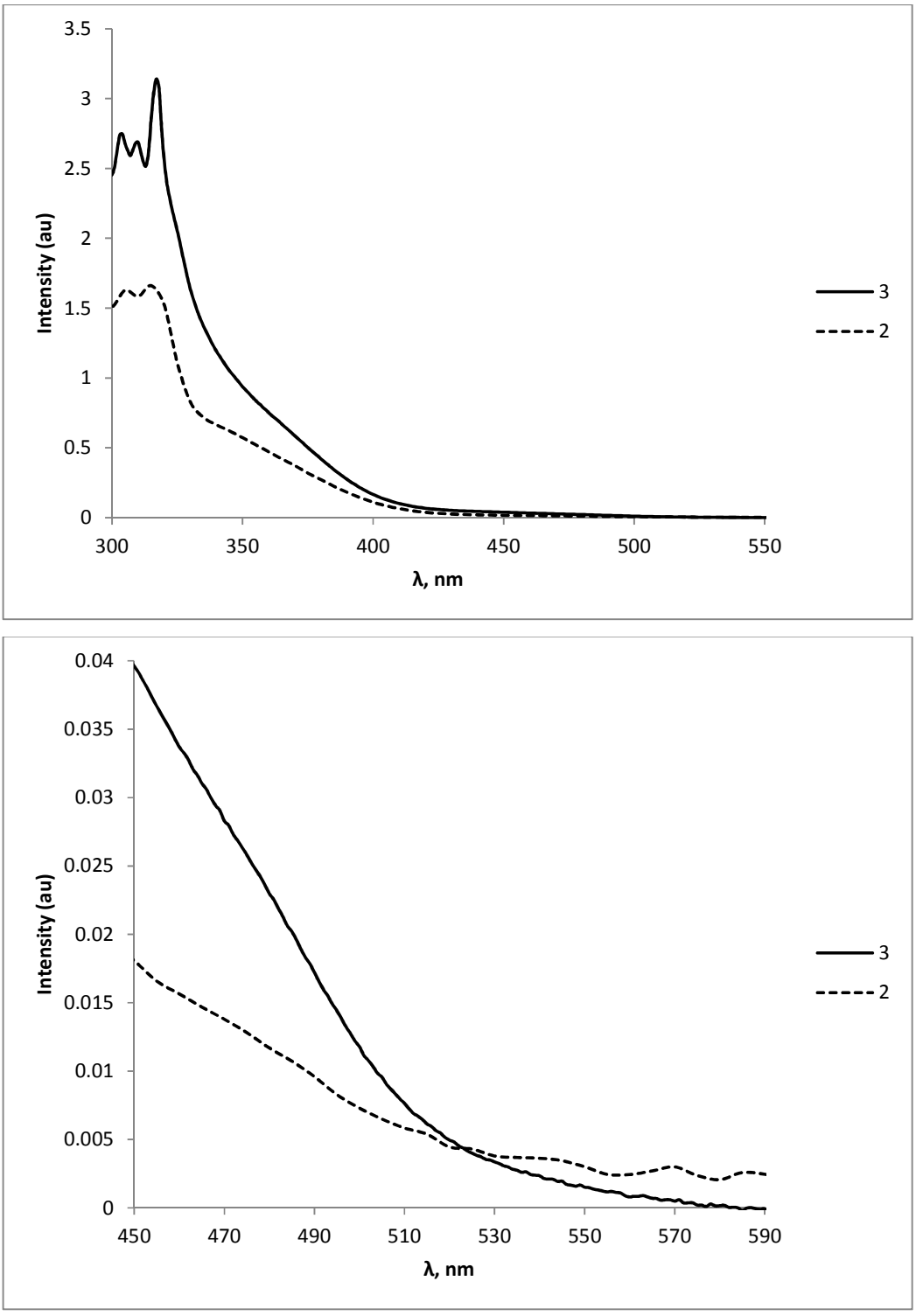

Fig. S1: UV-vis Spectra of 2 and 3

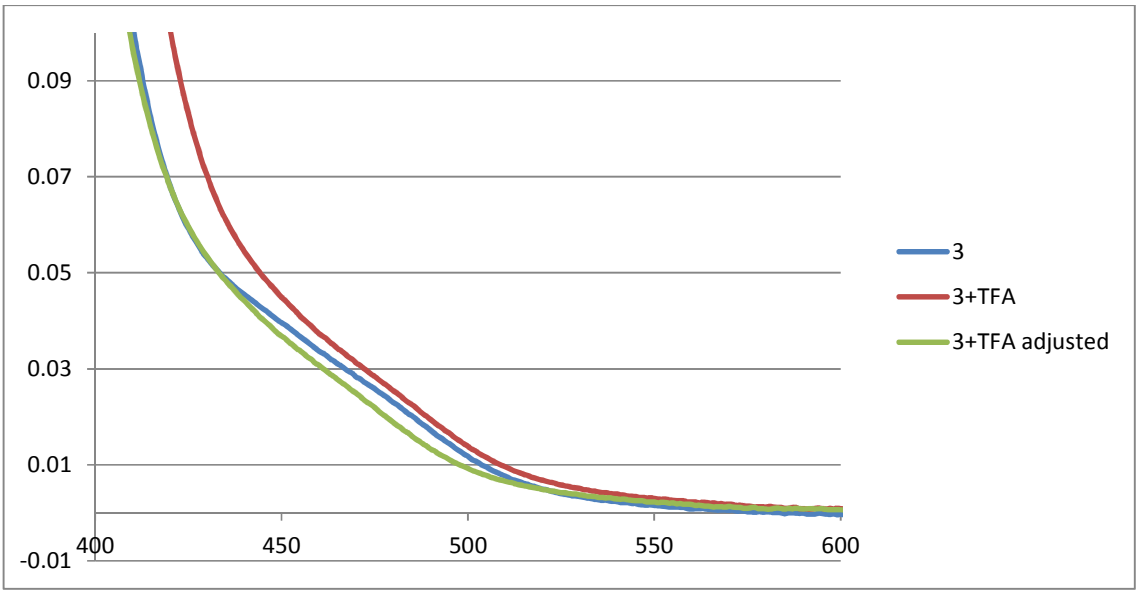

Fig. S2: UV-Vis absorbance spectrum of 3 with addition of TFA (showing red shift) and adjusted to overlap neutral spectrum showing loss of intensity of 450-500nm band.

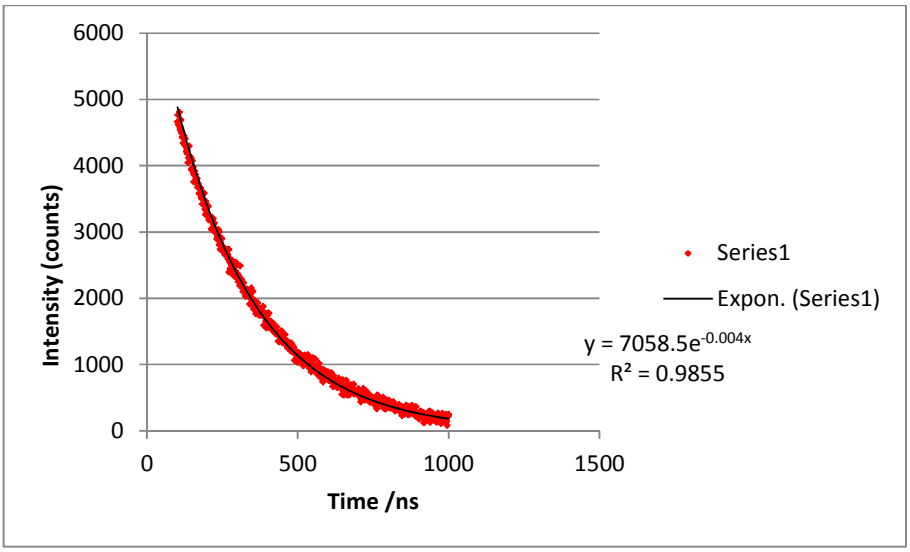

Fig. S3: Decay Plot for Lifetime Calculation for 2

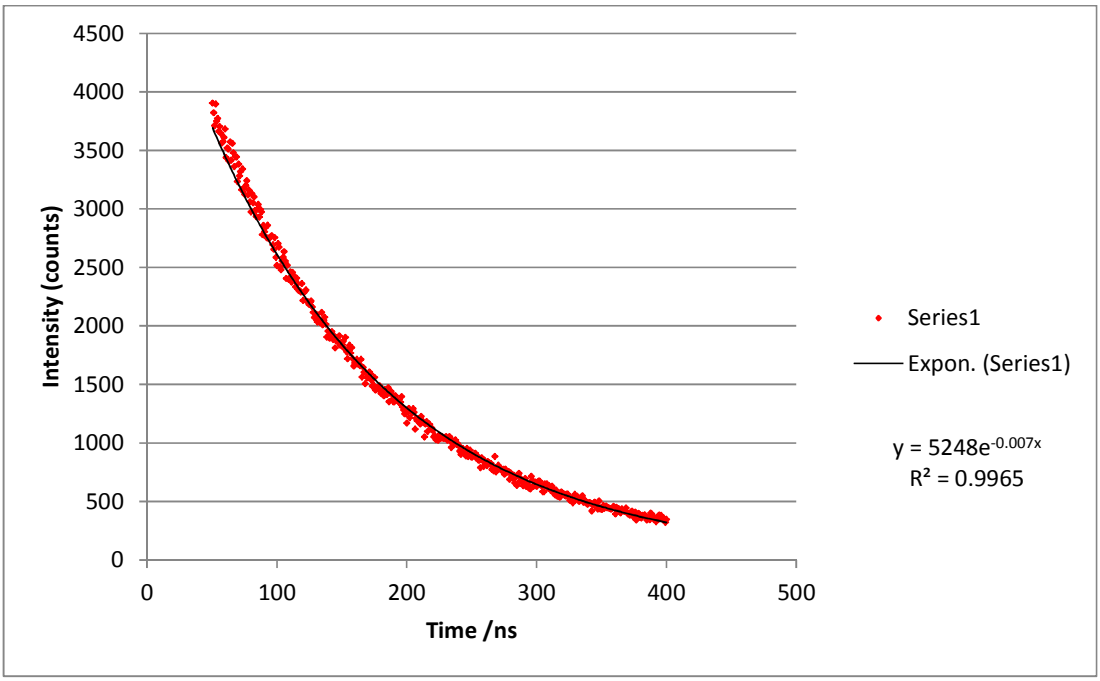

Fig. S4: Decay Plot for Lifetime Calculation for 3

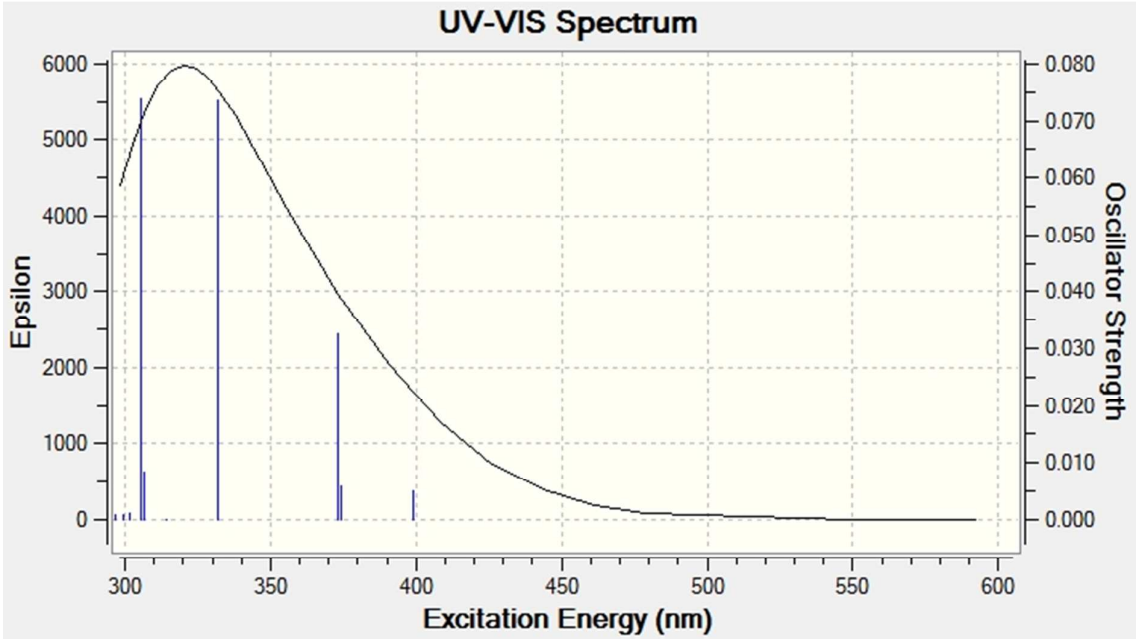

Fig S5: Simulated UV-Vis spectrum of 2.

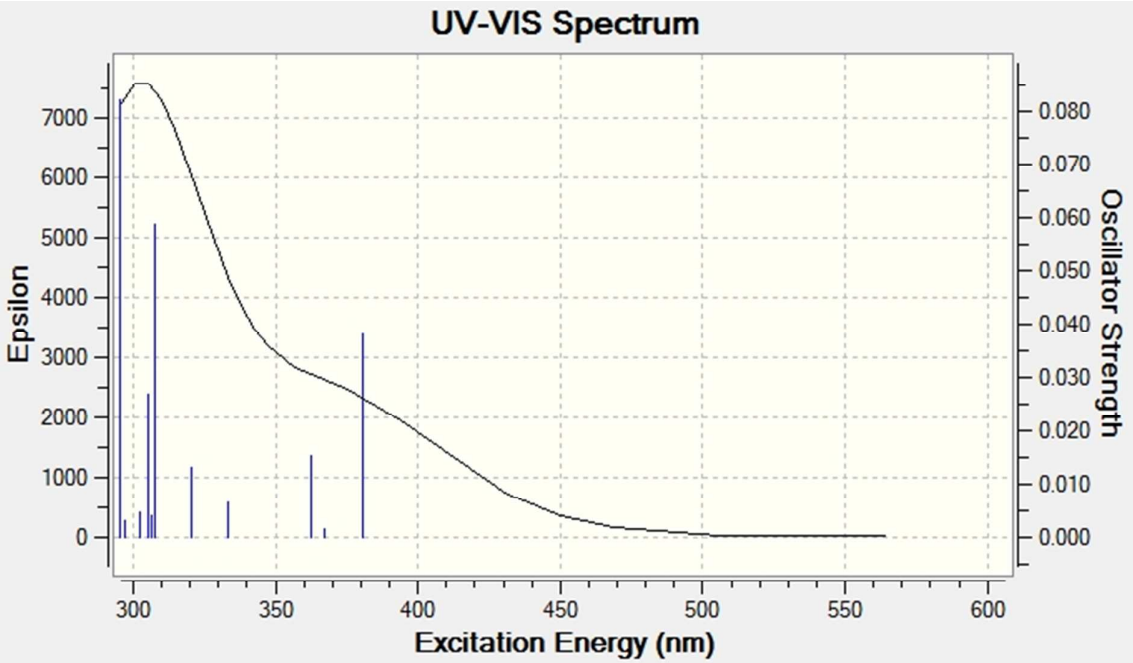

Fig. S6: Simulated UV-Vis spectrum of 3

Computational Details

All calculations were performed using Gaussian09,[3] using the B3LYP functional,[4] with Stuttgart-Dresden basis set and associated ECP on Re[5] and 6-31+G(d,p) on all remaining atoms.[6] Structures of individual complexes of **2** and **3** were extracted from the crystalline environment and fully geometry optimised within a polarizable continuum model (PCM) simulation of toluene. Calculation of absorption bands using TD-DFT, as well as frontier orbitals, were performed at this optimum geometry, again in PCM toluene.

Crystallographic Data

Data were collected by the EPSRC UK National Crystallography Service at the University of Southampton. Refinement was carried out using the SHELX program[7] in the WINGX package.[8] ORTEP 3[9] and POV-ray[10] programs were used for image generation.

Compound	**1**	**2**	**3**	**4**
Empirical formula	$C_{25}H_{26}N_4$	$C_{28}H_{26}BrN_4O_4Re$	$C_{28}H_{26}BrN_4O_3Re.(C_7H_8)$	$C_{25}H_{22}BrN_4O_3Re$
Formula weight	382.50	748.64	824.77	692.57
Temperature	100(2) K	100(2) K	100(2) K	100(2) K
Wavelength	0.71075 Å	0.71073 Å	0.71075 Å	0.71073 Å
Crystal system	Monoclinic	Triclinic	Triclinic	Monoclinic
Space group	*P* $2_1/n$	*P* -1	*P* -1	*P* $2_1/a$
Unit cell dimensions	a = 16.3443(11) Å b = 5.9490(4) Å c = 21.3716(15) Å α= 90.000° β= 106.773(3)° γ = 90.000°	a = 10.2026(7) Å b = 11.8088(8) Å c = 13.1060(9) Å α= 63.263(4)° β= 86.265(5)° γ = 73.684(4)°	a = 8.9603(5) Å b = 11.1814(8) Å c = 17.0562(11) Å α= 71.987(3)° β= 79.252(4)° γ = 86.961(4)°	a = 13.2087(9) Å b = 7.5055(5) Å c = 24.8936(18) Å α= 90.000° β= 104.400(5)° γ = 90.000°
Volume	1989.6(2) $Å^3$	1349.94(17) $Å^3$	1596.55(18) $Å^3$	2390.3(19) $Å^3$
Z	4	2	2	4
Density (calculated)	1.277 Mg/m^3	1.842 Mg/m^3	1.716 Mg/m^3	1.925 Mg/m^3
Absorption coefficient	0.077 mm^{-1}	6.022 mm^{-1}	5.098 mm^{-1}	6.790 mm^{-1}
F(000)	816	728	812	1336
Crystal size	0.36 x 0.06 x 0.04 mm^3	0.08 x 0.07 x 0.03 mm^3	0.23 x 0.09 x 0.04 mm^3	0.07 x 0.04 x 0.01 mm^3
Theta range for data collection	3.57 to 27.48°	2.456 to 27.510°	3.00 to 27.48°	2.843 to 27.484°
Index ranges	$-21 \le h \le 21$ $-6 \le k \le 7$ $-27 \le l \le 27$	$-13 \le h \le 13$ $-15 \le k \le 15$ $-15 \le l \le 16$	$-11 \le h \le 11$ $-14 \le k \le 14$ $-22 \le l \le 21$	$-17 \le h \le 17$ $-7 \le k \le 9$ $-30 \le l \le 32$
Reflections collected	17443	17641	21710	15745
Independent reflections	4497 [R_{int} = 0.0379]	6179 [R_{int} = 0.0282]	7305 [R_{int} = 0.0372]	5378 [R_{int} = 0.0385]
Completeness to theta = 27.48°	98.4 %	99.7 %	99.8 %	98.4 %
Absorption correction	Semi-empirical from equivalents	Semi-empirical from equivalents	Semi-empirical from equivalents	Semi-empirical from equivalents
Max. and min. transmission	1.000 and 0.774	1.000 and 0.774	1.000 and 0.763	1.000 and 0.694
Refinement method	Full-matrix least-squares on F^2	Full-matrix least-squares on F^2	Full-matrix least-squares on F^2	Full-matrix least-squares on F^2
Data / restraints / parameters	4497 / 0 / 268	6179 / 6 / 393	7305 / 0 / 404	5378 / 0 / 315
Goodness-of-fit on F^2	1.021	1.041	1.046	1.023
Final R indices [$I>2\sigma(I)$]	*R1* = 0.0387 *wR2* = 0.0927	*R1* = 0.0227, *wR2* = 0.0587	*R1* = 0.0233 *wR2* = 0.0591	*R1* = 0.0281 *wR2* = 0.0545
R indices (all data)	R1 = 0.0596 wR2 = 0.1019	*R1* = 0.0234 *wR2* = 0.0591	*R1* = 0.0243 *wR2* = 0.0597	*R1* = 0.0442 *wR2* = 0.0598
Largest diff. peak and hole	0.237 and -0.232 $eÅ^{-3}$	2.160 and -1.429 $eÅ^{-3}$	1.357 and -0.867 $eÅ^{-3}$	0.797 and -0.841 $eÅ^{-3}$

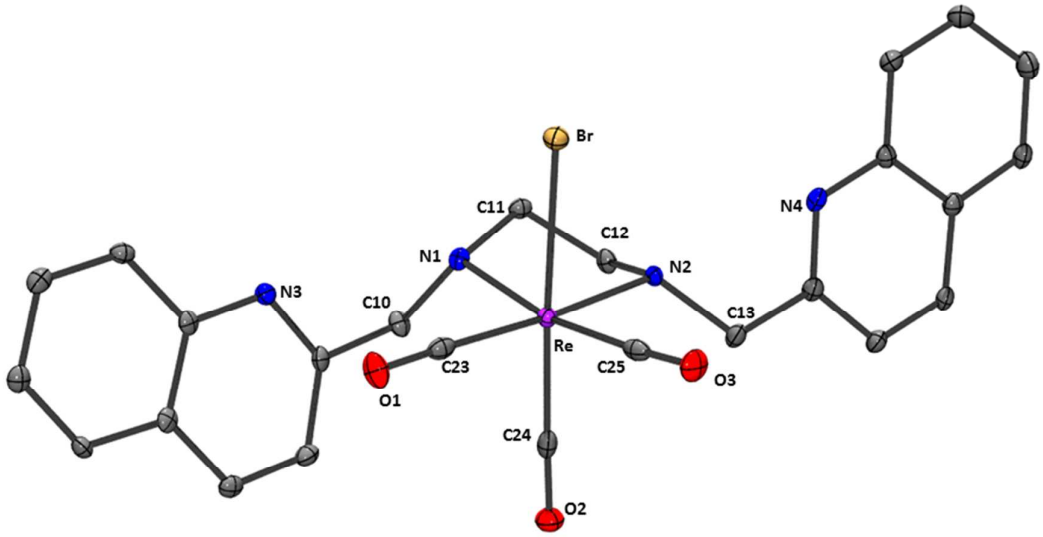

Fig. S7: Molecular Structure of Compound 4

References

1. S. P. Schmidt, W. C. Trogler, F. Basolo, *Inorg. Synth.*, 1990, **28**, 160.

2. V. Amendola, C. Mangano P. Pallavicini, *Dalton Trans.*, 2004, 2850.

3. Gaussian 09, Revision C.01, M. J. Frisch, G. W. Trucks, H. B. Schlegel, G. E. Scuseria, M. A. Robb, J. R. Cheeseman, G. Scalmani, V. Barone, B. Mennucci, G. A. Petersson, H. Nakatsuji, M. Caricato, X. Li, H. P. Hratchian, A. F. Izmaylov, J. Bloino, G. Zheng, J. L. Sonnenberg, M. Hada, M. Ehara, K. Toyota, R. Fukuda, J. Hasegawa, M. Ishida, T. Nakajima, Y. Honda, O. Kitao, H. Nakai, T. Vreven, J. A. Montgomery, Jr., J. E. Peralta, F. Ogliaro, M. Bearpark, J. J. Heyd, E. Brothers, K. N. Kudin, V. N. Staroverov, T. Keith, R. Kobayashi, J. Normand, K. Raghavachari, A. Rendell, J. C. Burant, S. S. Iyengar, J. Tomasi, M. Cossi, N. Rega, J. M. Millam, M. Klene, J. E. Knox, J. B. Cross, V. Bakken, C. Adamo, J. Jaramillo, R. Gomperts, R. E. Stratmann, O. Yazyev, A. J. Austin, R. Cammi, C. Pomelli, J. W. Ochterski, R. L. Martin, K. Morokuma, V. G. Zakrzewski, G. A. Voth, P. Salvador, J. J. Dannenberg, S. Dapprich, A. D. Daniels, O. Farkas, J. B. Foresman, J. V. Ortiz, J. Cioslowski, and D. J. Fox, Gaussian, Inc., Wallingford CT, 2010.

4. a) A. D. Becke, *J. Chem. Phys.*, 1993, **98**, 5648. b) C. Lee, W. Yang, R. G. Parr, *Phys. Rev. B*, 1988, **37**, 785.

5. a) D. Andrae, U. Haeussermann, M. Dolg, H. Stoll, and H. Preuss, *Theor. Chem. Acc.*, 1990, **77**, 123. b) R. Ditchfield, W. J. Hehre, J. A. Pople, *J. Chem. Phys.*, 1971, **54**, 724. c) P. C. Hariharan and J. A. Pople, *Theor. Chem. Acc.*, 1973, **28**, 213.

6. J. Tomasi, B. Mennucci, R. Cammi, *Chem. Rev.*, 2005, **105**, 2999 and references cited therein.

7. G.M. Seldrick, *Acta Crystallogr.*, A64, 2008, 112.

8. L. J. Farrugia *J. Appl.Cryst.*, 1999, **32**, 837.

9. Michael N. Burnett and Carroll K. Johnson, ORTEP-III: Oak Ridge Thermal Ellipsoid Plot Program for Crystal Structure Illustrations, Oak Ridge National Laboratory Report ORNL-6895, 1996.
10. Persistence of Vision Pty. Ltd. (2004), Persistence of Vision Raytracer (Version 3.6) [Computer software]. Retrieved from http://www.povray.org/download/

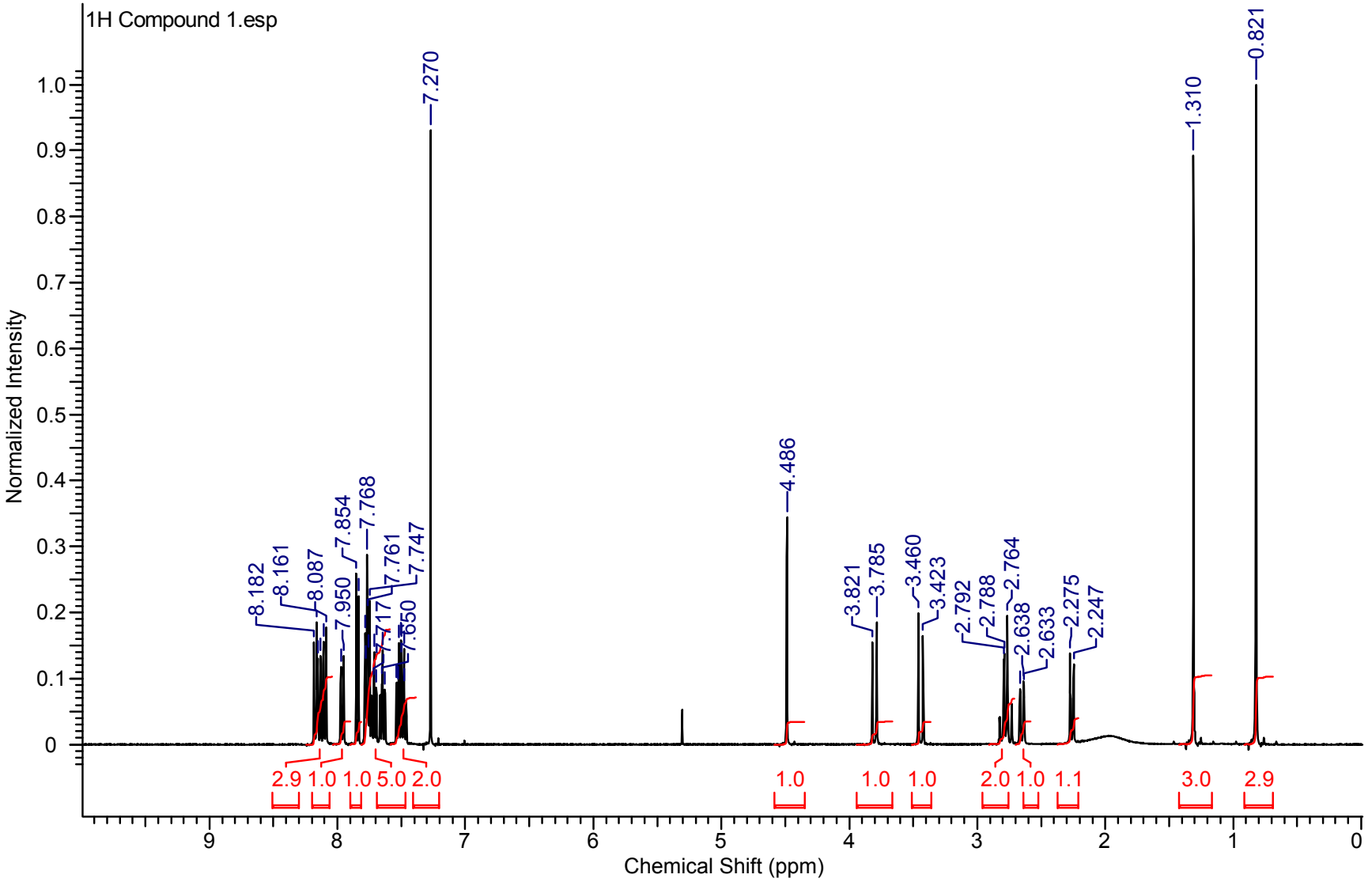
1H Compound 1.esp
Normalized Intensity
Chemical Shift (ppm)
8.182
8.161
8.087
7.950
7.854
7.768
7.761
7.747
7.717
7.650
7.270
4.486
3.821
3.785
3.460
3.423
2.792
2.788
2.764
2.638
2.633
2.275
2.247
1.310
0.821
2.9 1.0 1.0 5.0 2.0
1.0 1.0 1.0 2.0 1.0 1.1 3.0 2.9

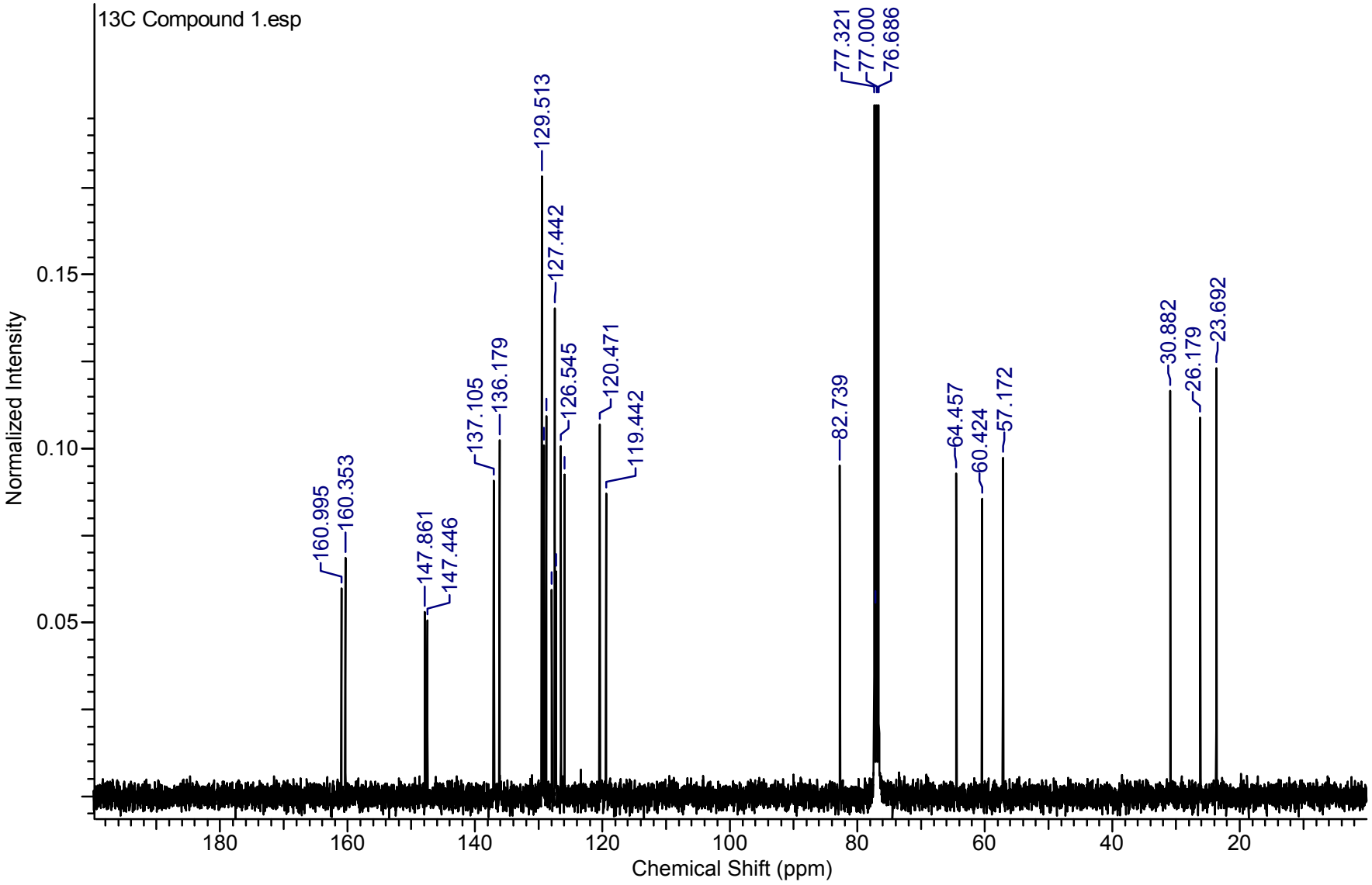
13C Compound 1.esp
Normalized Intensity
0.15
0.10
0.05
160.995
160.353
147.861
147.446
137.105
136.179
129.513
127.442
126.545
120.471
119.442
82.739
77.321
77.000
76.686
64.457
60.424
57.172
30.882
26.179
23.692
180
160
140
120
100
80
60
40
20
Chemical Shift (ppm)

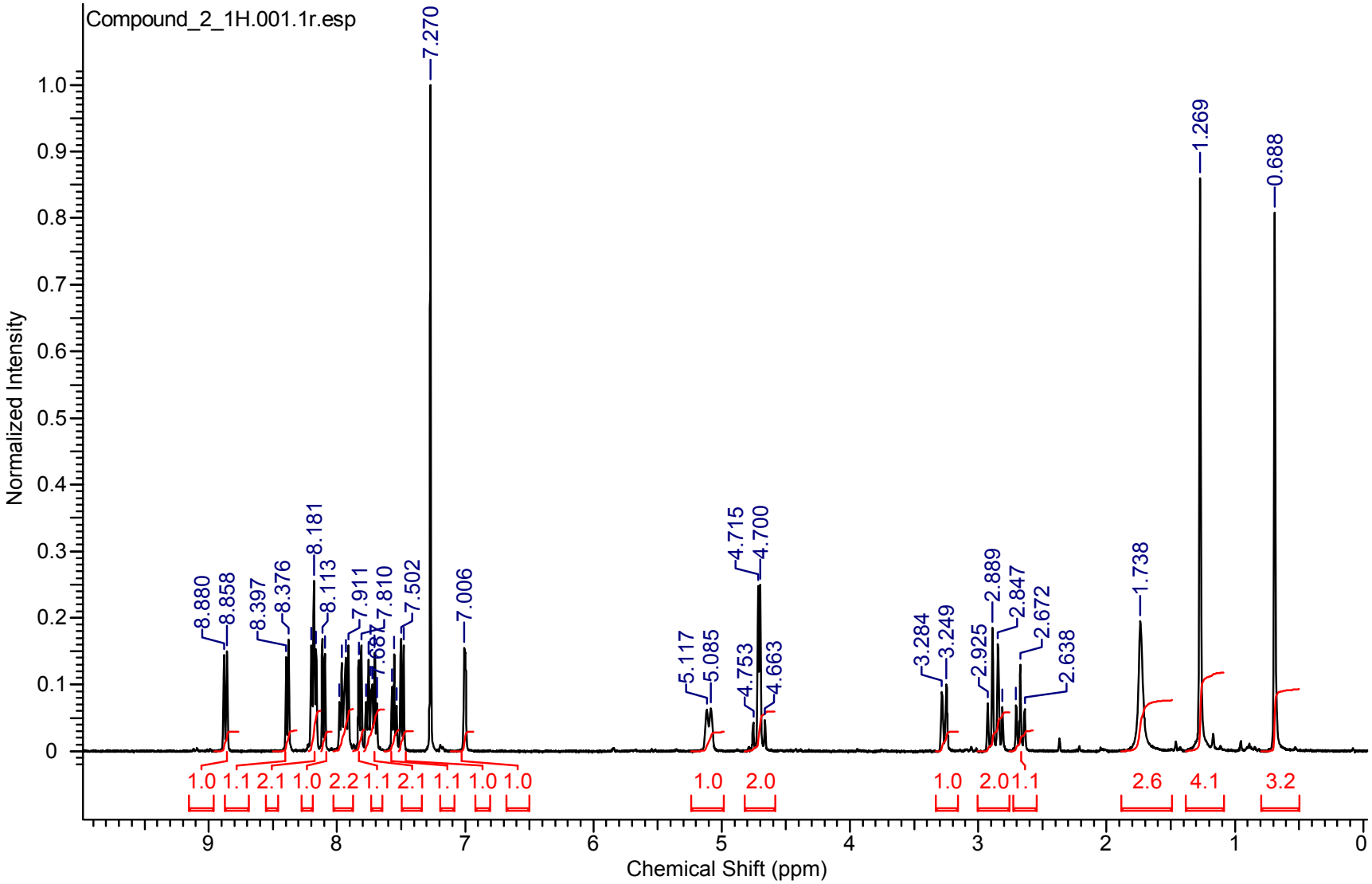
Compound_2_1H.001.1r.esp
Normalized Intensity
Chemical Shift (ppm)
8.880
8.858
8.397
8.376
8.181
8.113
7.911
7.810
7.687
7.502
7.270
7.006
5.117
5.085
4.753
4.715
4.700
4.663
3.284
3.249
2.925
2.889
2.847
2.672
2.638
1.738
1.269
0.688
1.0 1.1 2.1 1.0 2.2 1.1 2.1 1.1 1.0 1.0
1.0 2.0
1.0 2.0 1.1
2.6
4.1
3.2

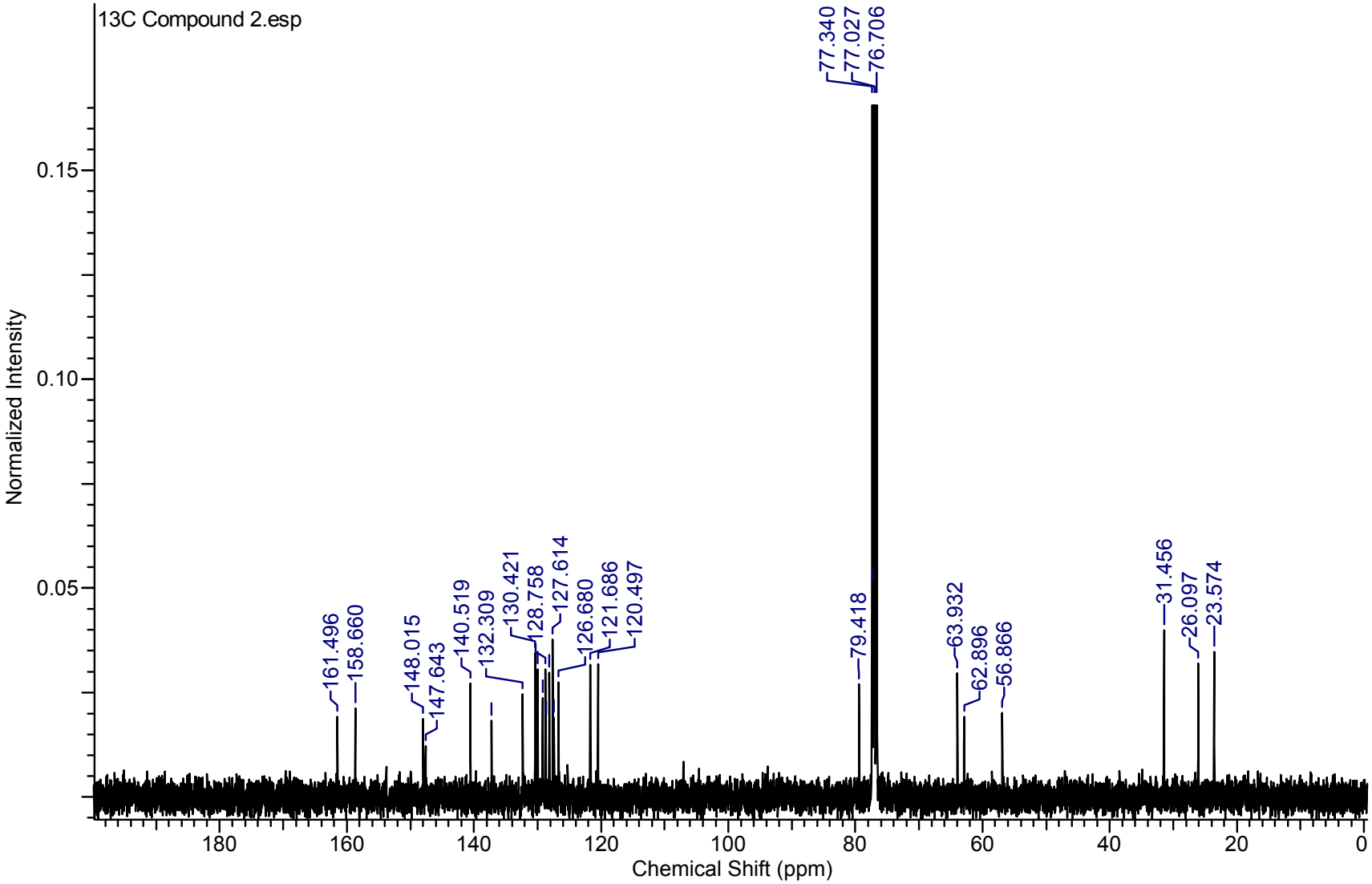
13C Compound 2.esp
Normalized Intensity
0.15
0.10
0.05
77.340
77.027
76.706
161.496
158.660
148.015
147.643
140.519
132.309
130.421
128.758
127.614
126.680
121.686
120.497
79.418
63.932
62.896
56.866
31.456
26.097
23.574
180
160
140
120
100
80
60
40
20
0
Chemical Shift (ppm)

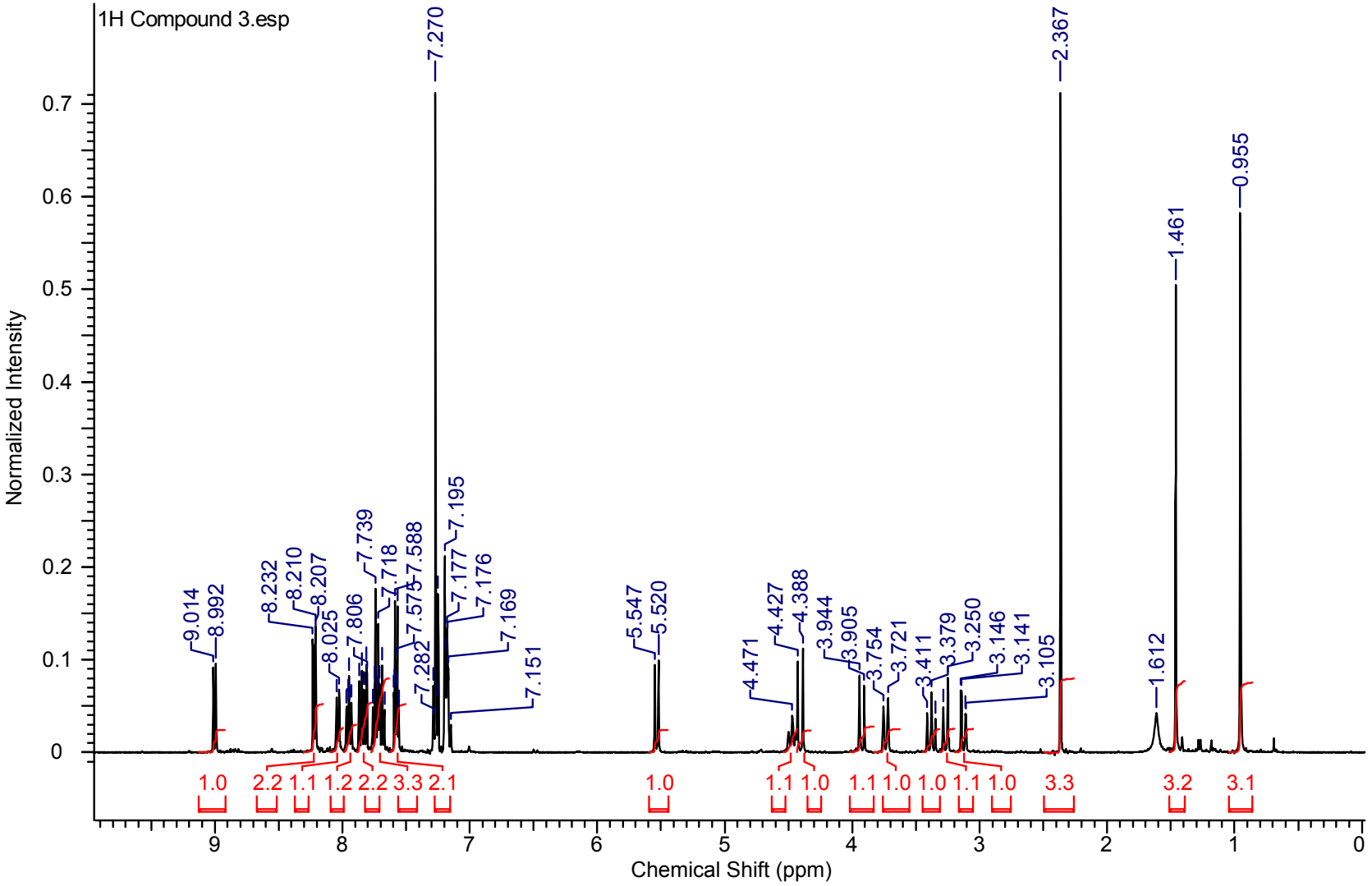
1H Compound 3.esp
Normalized Intensity
Chemical Shift (ppm)
9.014
8.992
8.232
8.210
8.207
8.025
7.806
7.739
7.718
7.588
7.575
7.282
7.270
7.195
7.177
7.176
7.169
7.151
5.547
5.520
4.471
4.427
4.388
3.944
3.905
3.754
3.721
3.411
3.379
3.250
3.146
3.141
3.105
2.367
1.612
1.461
0.955
1.0 2.2 1.1 1.2 2.2 3.3 2.1 1.0 1.1 1.0 1.1 1.0 1.0 1.1 1.0 3.3 3.2 3.1

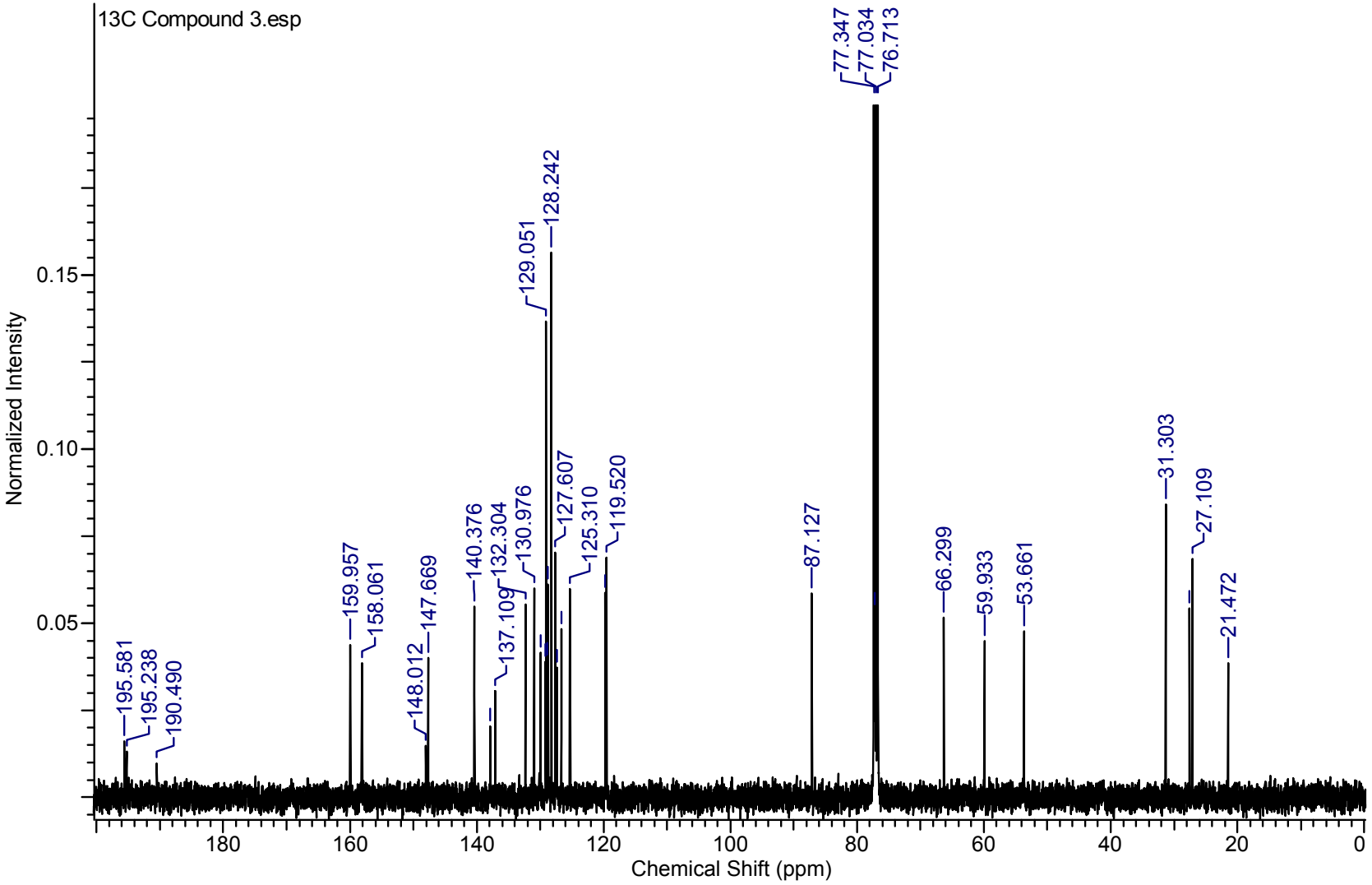
13C Compound 3.esp
Normalized Intensity
0.15
0.10
0.05
195.581
195.238
190.490
159.957
158.061
148.012
147.669
140.376
137.109
132.304
130.976
129.051
128.242
127.607
125.310
119.520
87.127
77.347
77.034
76.713
66.299
59.933
53.661
31.303
27.109
21.472
180
160
140
120
100
80
60
40
20
0
Chemical Shift (ppm)

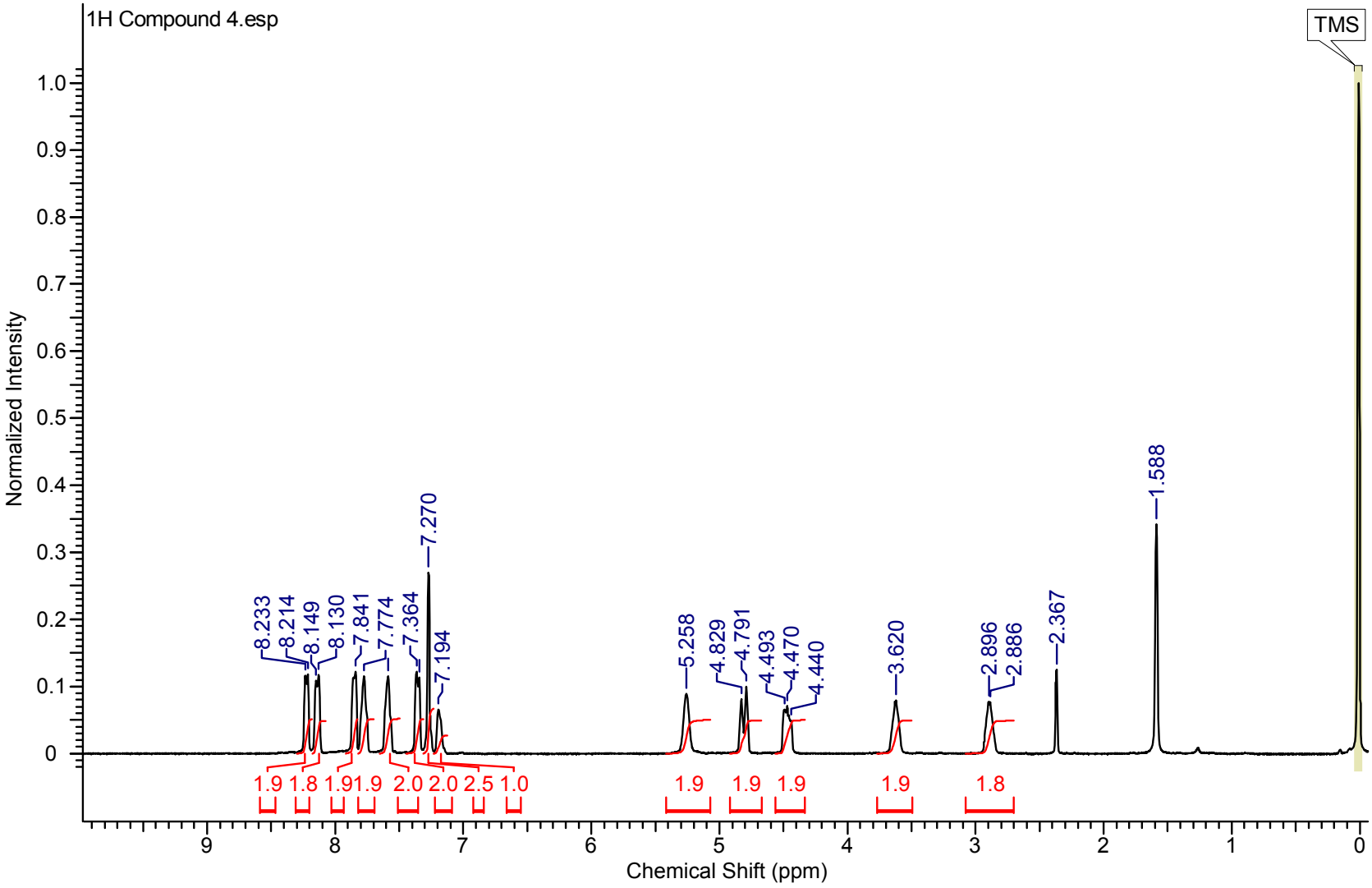
1H Compound 4.esp
TMS
Normalized Intensity
Chemical Shift (ppm)
8.233
8.214
8.149
8.130
7.841
7.774
7.364
7.270
7.194
5.258
4.829
4.791
4.493
4.470
4.440
3.620
2.896
2.886
2.367
1.588
1.9 1.8 1.9 1.9 2.0 2.0 2.5 1.0
1.9 1.9 1.9 1.9 1.8

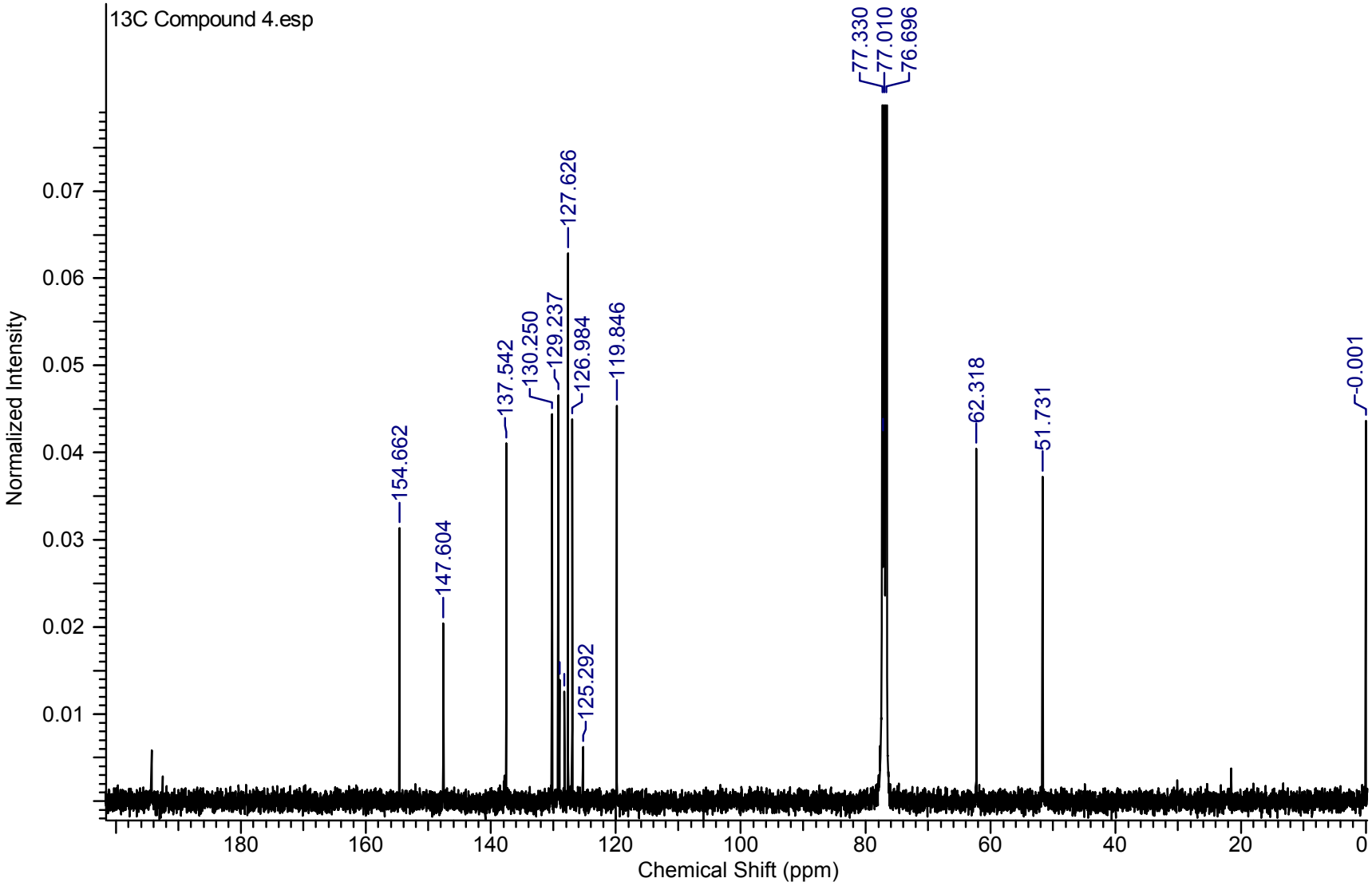
13C Compound 4.esp
Normalized Intensity
0.07
0.06
0.05
0.04
0.03
0.02
0.01
154.662
147.604
137.542
130.250
129.237
127.626
126.984
125.292
119.846
77.330
77.010
76.696
62.318
51.731
-0.001
180
160
140
120
100
80
60
40
20
0
Chemical Shift (ppm)

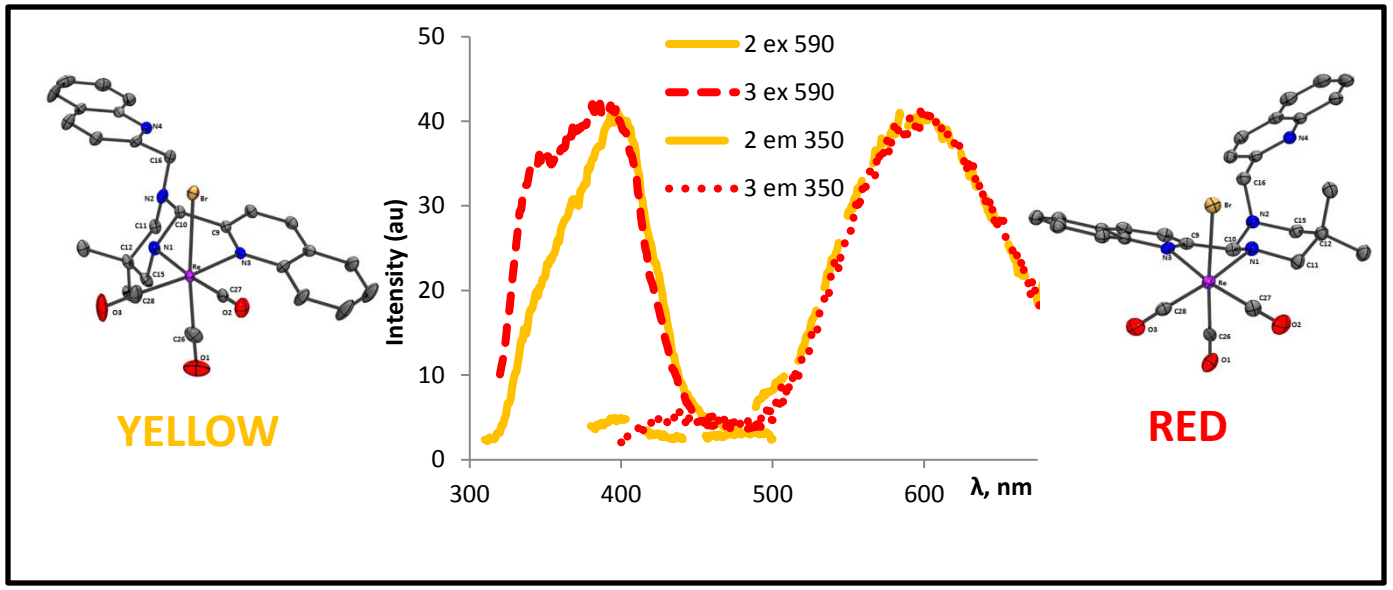
YELLOW
Intensity (au)
50
40
30
20
10
0
300
400
500
600
λ, nm
2 ex 590
3 ex 590
2 em 350
3 em 350
RED